

Chapter 9

Geomagnetic Storms



phys.org

www.skywave-radio.org

9 Geomagnetic Storms

Erratic fluctuations in Earth's magnetic field are classified as geomagnetic storms. Erratic fluctuations in the ionosphere's absorption levels and critical frequencies are called ionospheric storms. Both types of fluctuations are caused by dynamic solar winds impacting Earth's magnetosphere, in addition to the occurrence of solar flares. Geomagnetic and ionospheric storms are completely different things even though they are caused by the same solar events. This chapter focuses on geomagnetic storms. Ionospheric storms are the subject of Chapter 19

In addition to global geomagnetic storms, there are also substorms. Geomagnetic substorms are short duration storms that occur within the Earth's polar regions. A major global geomagnetic storm usually has associated with it a number of auroral substorms. However, the reverse is not true. Substorms may appear on their own when there are no mid or low latitude storms. Auroral substorms typically occur at a rate of about 4 per day during the solar cycle declining phase. Auroral borealis sightings are also most prevalent during this phase of the solar cycle.

Geomagnetic storms can seriously disrupt electrical power distribution grids causing millions of people to lose electrical power for several hours to a few months. Geomagnetic storms also induce dangerous electric currents into long pipelines, affect airline travel on routes over the polar regions, increase satellite drag accelerating satellite end of life, and affect many other aspects of our technological world. The most severe geomagnetic storm on record occurred in 1859 seriously disrupting telegraph communications. It is estimated that a storm of that magnitude occurring today would cause over \$2 trillion in damages.

Magnetic storms have been known since the eighteenth century, but not by the current name. They were first noticed as unexplained fluctuations in compass needles. Our current understanding of magnetic storms has come from continuous monitoring of Earth's magnetic field using magnetometers augmented by extensive measurements from spacecraft in Earth orbit. Magnetometer records over the past 150 years clearly show the sporadic occurrence and intensity of magnetic storms. The Earth's magnetic field has been, and continues to be, intensively studied from spacecraft beginning with the first Earth satellite (Explorer 1) launched by the United States in January 1958.

9.1 What Causes a Geomagnetic Storm

Earth's magnetic field is considered quiet when its amplitude and phase vary smoothly with time in an expected way. Under quiet conditions, the solar wind blows calmly along the magnetosheath, the Interplanetary Magnetic Field (IMF) has little or no southward component, the plasma sheet is calm, and the magnetosphere as a whole is undisturbed.

A geomagnetic storm occurs when a solar wind with a southward directed IMF impacts Earth's magnetosphere. Magnetic storms can also occur when a northward directed IMF solar wind encounters the magnetosphere. But such storms, if they occur at all, are small compared to storms triggered by southward directed IMF solar winds.

North and south is measured in terms of the Geocentric Solar Magnetospheric (GSM) coordinate system. This system, shown in Figure 1, is considered the best coordinate system to use when studying the effects of solar wind IMF on Earth's magnetosphere. The GSM coordinate system, centered on the Earth (geocentric), is defined relative to Earth's magnetic field axis. The radial x-axis (X_{GSM}) points from the center of the Earth to the center of the Sun. The z-axis (Z_{GSM}) is aligned with Earth's magnetic field axis and the y-axis (Y_{GSM}) is perpendicular to both the x and z axis.

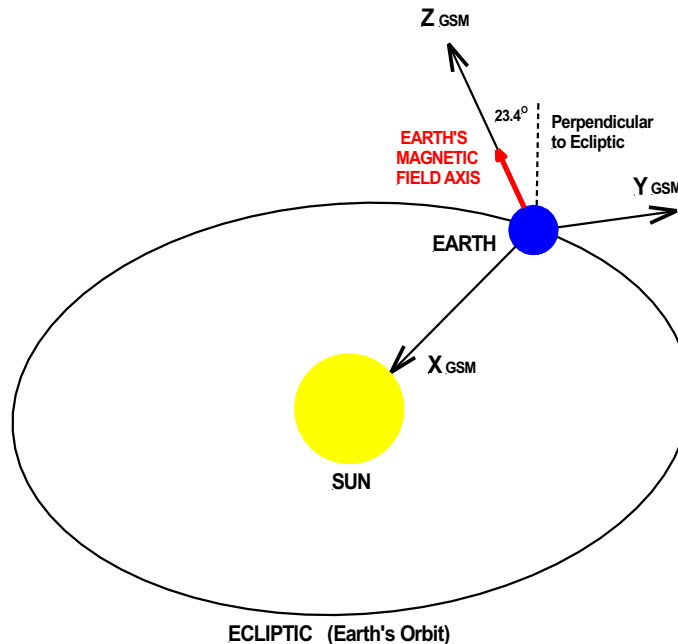


Figure 1 Geocentric Solar Magnetospheric (GSM) Coordinates (source: author)

In Figure 2 a southward directed ($-Z_{GSM}$) IMF encounters Earth's northward ($+Z_{GSM}$) magnetic field on the sunward side of the magnetosphere. The oppositely directed magnetic field lines cancel each other forming a magnetic neutral point, the red rectangle adjacent to the bow shock in Figure 2. Neither field exists within the neutral point. Consequently, each field line is broken as it enters the neutral region. Above and below the neutral point the "broken" IMF and geomagnetic field lines reconnect, but this time to each other as illustrated in Figure 3. In this figure the field line marked 1' is an IMF field line just as it is about to cancel with geomagnetic field line 1. Field line 2 represent the two broken field lines after they have reconnected forming a single unified line.

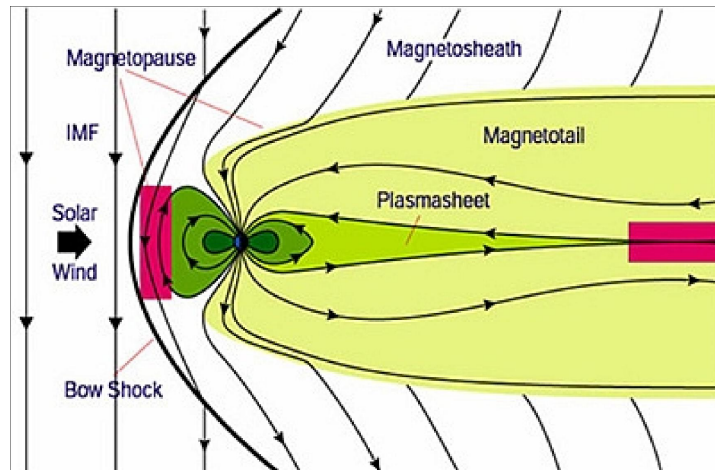


Figure 2 Magnetic neutral points (source: Satellite Missions)

However, a problem arises with this reconnection. The IMF is “frozen in” the solar wind and thus moves with the wind. As it does so it drags Earth’s connected magnetic field lines along with it over the poles from the day to night side of the magnetosphere. In addition, connection to the IMF peels open the geomagnetic field lines over the polar regions allowing a flood of solar wind charged particles to flow down the field lines into Earth’s inner magnetosphere. The inflow of charged particles increase the strength of the equatorial ring current leading directly to a geomagnetic storm. How strong the storm is depends on the speed and particle density of the solar wind at the time. High speed solar wind streams created by coronal holes, coronal mass ejections, solar flares, solar energetic particles (SEPs), in addition to corotating wind interaction regions near the Earth can all increase the speed and density of the solar wind, increasing the severity of a geomagnetic storm. The Solar Wind chapter describes these solar events in considerable detail. The equatorial ring current circles the Earth above the magnetic equator in the region of the Van Allen radiation belts 2 to 6 Earth radii from the center of the Earth, as described in the previous chapter. In Figure 4 the ring current is illustrated by positively charged protons drifting westward around the Earth and negatively charged electrons circulating eastward.

After being dragged over the polar region, the unified IMF - geomagnetic field collapses part way out in the magnetosphere tail forming a magnetic neutral region. This neutral point is illustrated in Figure 2 by the red rectangle on the right side of the figure. The magnetic field disappears in the neutral zone meaning that the unified IMF – geomagnetic field lines are broken. The field lines on the Earth side of the neutral zone reconnect as closed geomagnetic field line that flow back to Earth (field line 6 in Figure 3). Field lines on the far side of the neutral zone reconnect as IMF field lines (field line 7’). These field lines are carried by the solar wind away from Earth out into the far reaches of the magnetotail where they eventually rejoin the main part of the IMF.

In the process plasma in Earth’s ionosphere is dragged across Earth’s polar region from the day to night side of the Earth (1 through 6 shown in the Figure 3 insert). The plasma flows back toward the

day side of the Earth at latitudes below the auroral zone as the geomagnetic field breaks away from the IMF and loops back to Earth (7 through 9 in Figure 3).

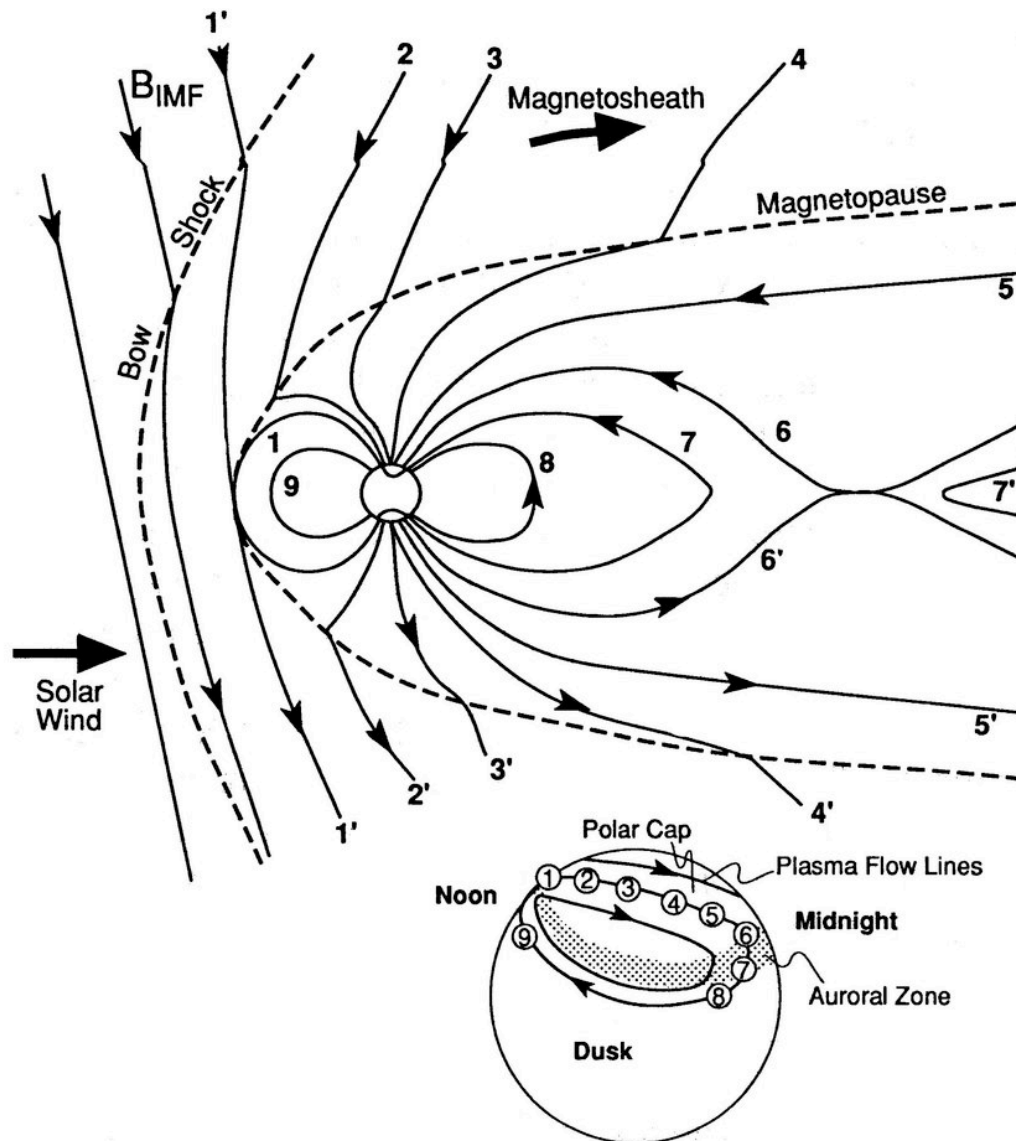


Figure 3 Dungey convection cycle (source: ResearchGate)

Dragging of the geomagnetic field across the polar regions of the Earth combined with the associated plasma flows is known as the Dungey convection cycle. British scientist James Dungey proposed the cycle in 1961 to explain the interaction between Earth's magnetosphere and the solar wind.

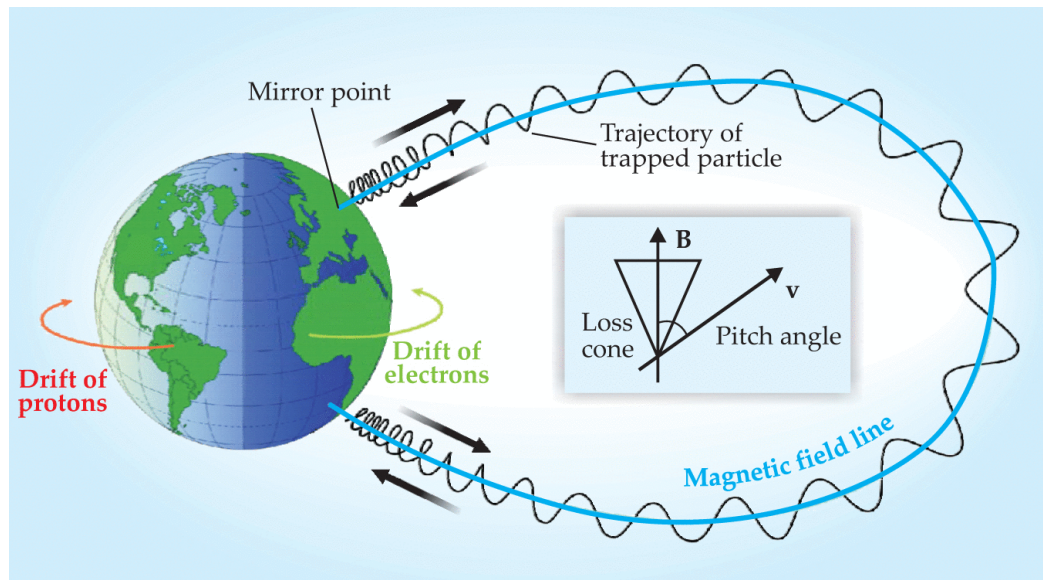


Figure 4 Trapped Charged Particles (source: Physics Today – Scitation)

The Dungey convection cycle does not occur with a north directed IMF. A north directed IMF (Figure 5) is parallel to the geomagnetic field. Consequently, a magnetic neutral point on the day side of the magnetosphere, with its corresponding magnetic reconnections, does not occur. Since the two fields do not break and reconnect, Earth's magnetic field (D in Figure 5) remains primarily a closed field.

Geomagnetic storms can occur during a north directed IMF if the speed and density of the solar wind is great enough. However, the magnitude of such storms are generally small since the geomagnetic field lines remain closed minimizing the inflow of solar wind particles into the inner magnetosphere.

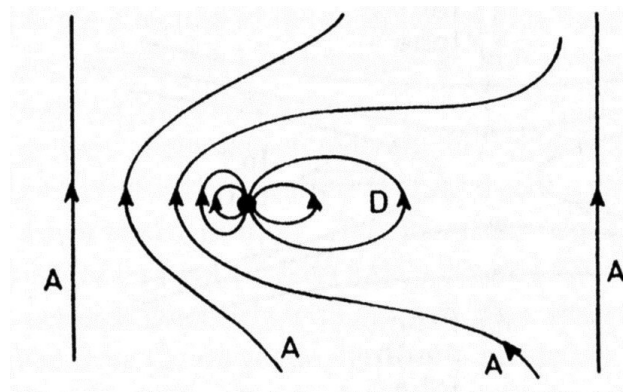


Figure 5 North Directed IMF (source Hunsucker)

9.2 Factors Effecting The Occurrence and Strength of Geomagnetic Storms.

Throughout the 11 year solar cycle various solar events occurring in different regions of the Sun produce the solar winds responsible for creating geomagnetic storms. These events include:

- Prominences,
- Coronal loops,
- Coronal helmet streamers and substreamers,
- Coronal holes,
- Solar flares
- Coronal Mass Ejections (CMEs), and

9.2.1 Solar Cycle

As we know, the solar cycle is the result of the Sun's differential rotation rate (the Sun's equator rotates faster than its poles) coupled with its magnetic field being formed in the outer part of the Sun, specifically in the convection zone just below the photosphere. The photosphere is what we perceive as the Sun's surface (Figure 6).

During solar minimum few if any sunspots are visible on the Sun. The Sun's magnetic field is a "quiet" north – south bipolar field (Figure 7a) with a magnetic field strength of about 1.0 gauss, not much different from Earth's magnetic field.

However, over a period of 3 to 6 years the Sun's differential rotation drags and winds the magnetic field around the Sun as shown in Figure 7 "a" through "c". The magnetic field at the equator is dragged around the Sun faster than the magnetic field at the poles winding the original bipolar field in Figure 7a into the toroidal field shown in Figure 7c. In addition, convection zone turbulence twists the magnetic field lines into ropes some of which become knotted.

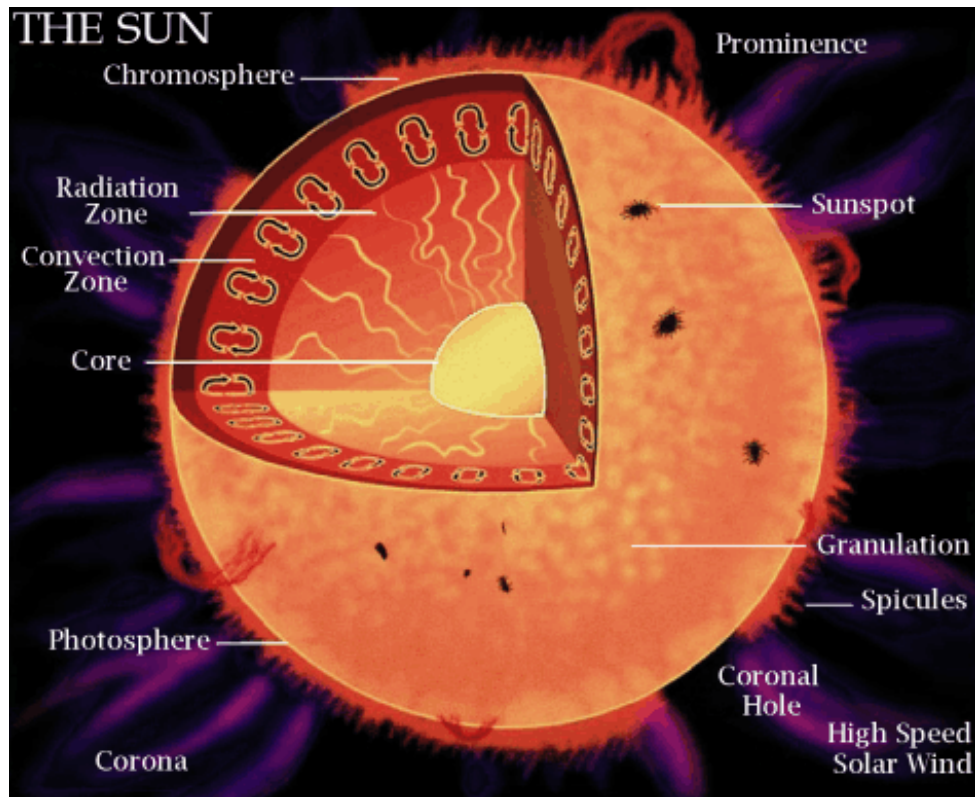


Figure 6 The Sun (source: NASA).

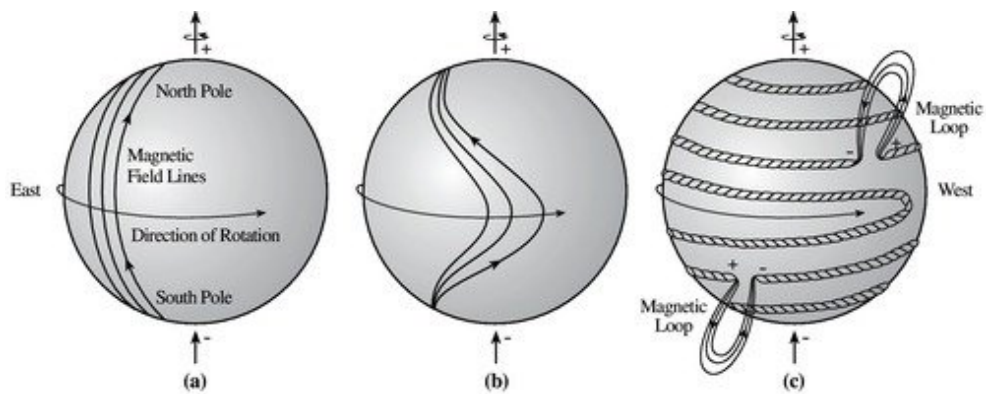


Figure 7 Twisted magnetic field lines (source: NASA's Cosmos – ase.tufts.edu)

Winding the magnetic field around the Sun in tighter ever increasing number of turns is not a sustainable process. Something has to break, and it does! Continued winding, twisting, and

knotting creates tremendous stress in the magnetic field driving field intensities to well over 3,000 gauss.

The enormous stress eventually causes the field to rupture in many places. As it does so high arching prominences, coronal loops (magnetic loops in Figure 7c), sunspots, and solar flares erupt from the Sun. The Sun reaches solar maximum during this very turbulent phase of the solar cycle with large numbers of sunspots visible on the solar surface.

As the magnetic field disintegrates, sunspots gradually disappear and the Sun again approaches solar minimum with a quiet north-south magnetic field.

In the literature, the solar cycle is described as having four phases illustrated in Figure 8:

- Solar minimum: few if any sunspots visible,
- Ascending phase: a few sunspots appearing near 30° solar latitudes (Figure 9),
- Solar Maximum: Sun very active with large numbers of sunspots at lower latitudes,
- Declining phase: Sunspots gradually move toward the Sun's equator and disappear

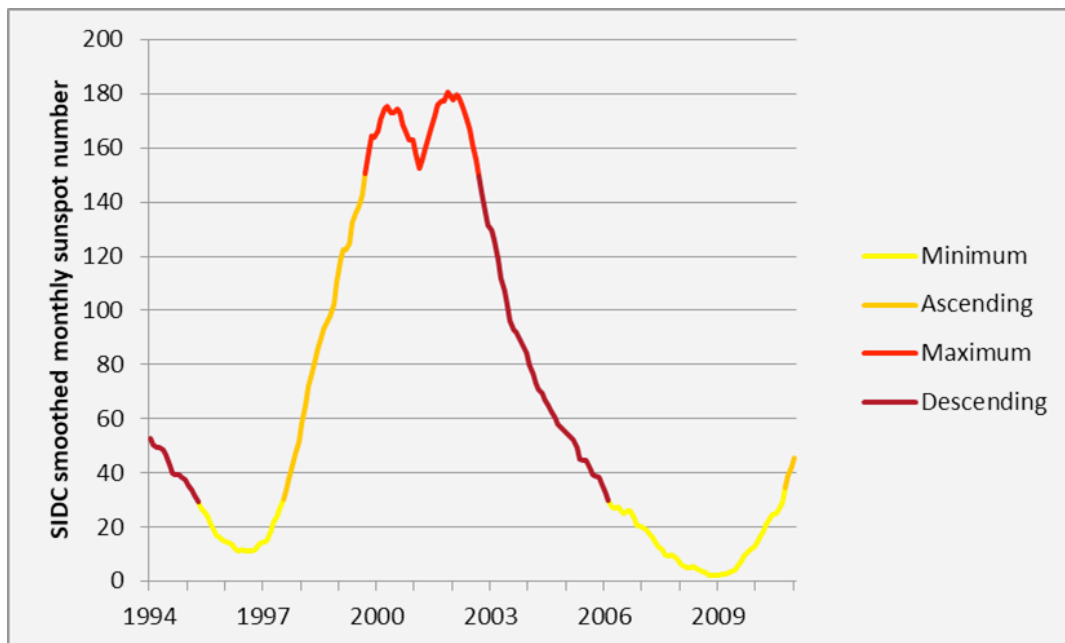


Figure 8 Solar cycle phases (source: STCE)

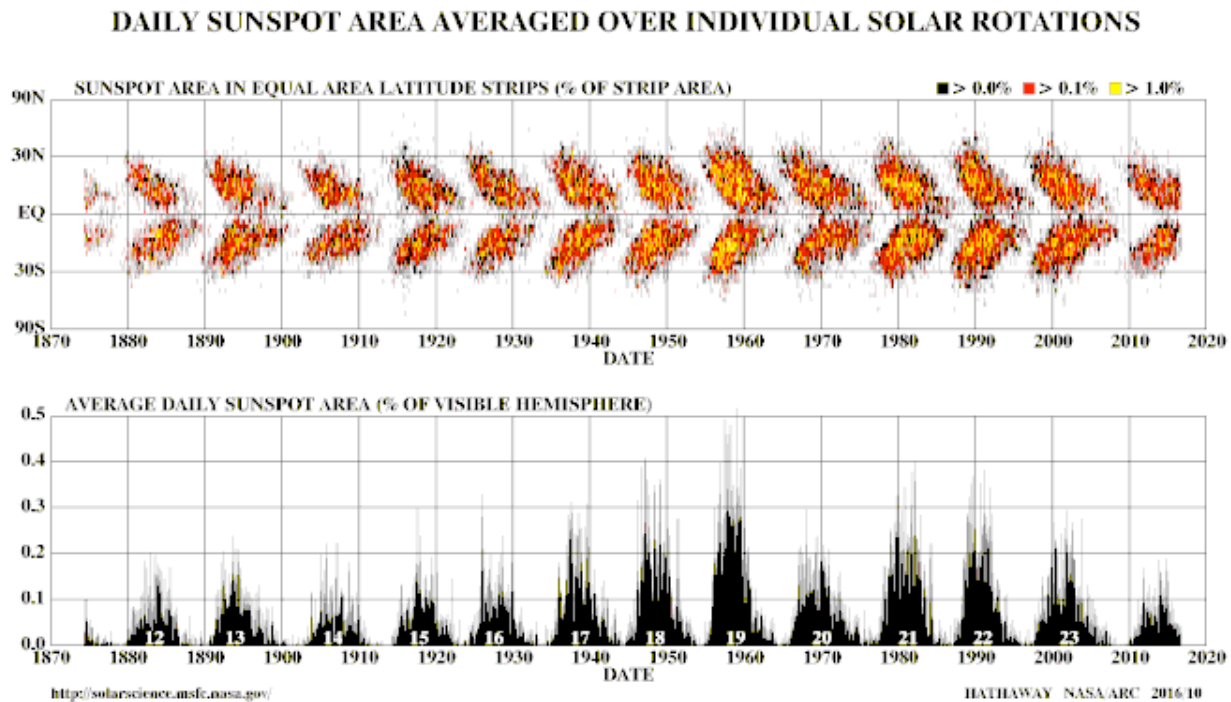


Figure 9 Solar cycle sunspot activity (source: Hathaway)

9.2.2 Prominence

Prominences are bright loops (Figure 10 left) and curtains (Figure 10 right) of relatively cool plasma suspended above the photosphere by strong arching magnetic fields. In addition to plasma, prominences contain neutral hydrogen atoms which emit light in the H_{α} spectrum when the electron of a hydrogen atom is excited to a higher energy level and then falls back to its initial state. Prominences are often but not always associated with sunspot regions.

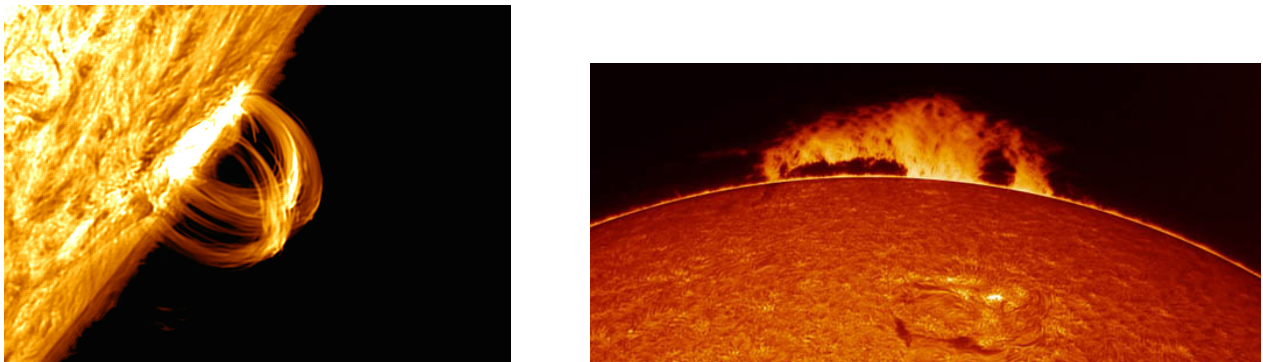


Figure 10 Solar Prominence (source: Astronomy Magazine)

A prominence occurs when the Sun's stressed magnetic field erupts through the photosphere carrying with it electrically charged plasma. The charged plasma, often traveling at speeds of 40 km/sec, follows the contours of the magnetic field giving a prominence its bright arching shape. The strength of the magnetic field within a prominence typically ranges from 10 to 800 gauss, compared to the Sun's quiet bipolar field of around 1 gauss and intensities of over 3,000 gauss in magnetic field lines that become twisted and knotted. A prominence extends into the corona often 50,000 km or more above the photosphere and usually lasts for several hours. In some cases a prominence can remain in place for 2 - 3 solar rotations (~ 1 to 3 months). The temperature within a prominence is on the order of 7,000 degrees kelvin, much cooler and more dense than the surrounding corona. The stability of a prominence is due to the equilibrium between its opposing magnetic and gravitational forces. Disruption of this equilibrium causes prominences to collapse, sometimes catastrophically producing solar flares and coronal mass ejections.

Bright loop prominences (Figure 10 left) occur in active regions of the Sun, particularly during solar maximum. In contrast, curtain prominences (Figure 10 right) are generally found far from active regions.

9.2.3 Coronal Loops

Coronal loops are markedly different from prominences. Coronal loops are created by upwelling magnetic fields generated inside the Sun with their foot points anchored in the photosphere, similar to prominences. But unlike prominences, coronal loops are much larger extending far out into the corona, as illustrated in Figures 11 and 12. The size of the Earth relative to a coronal loop is illustrated in Figure 11. Coronal loops often form above sunspot groups in the active regions of the Sun magnetically connecting one region on the solar surface to another.



Figure 11 Coronal loop (source: NASA's Cosmos)

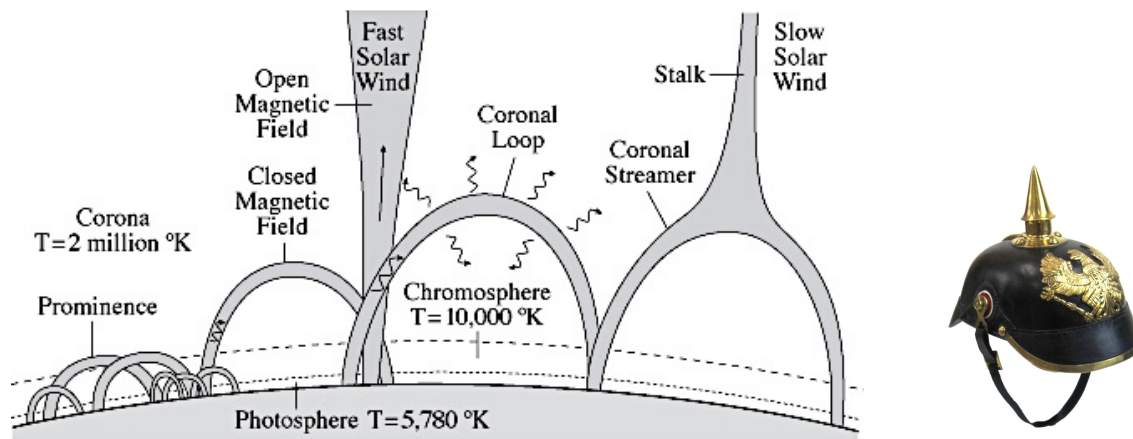


Figure 12 Prominence, Coronal Loops, & Streamers (source: NASA)

The plasma filling a coronal loop is much hotter than in a prominence. Because of its high temperature, a coronal loop can not emit light from neutral hydrogen atoms. At coronal loop temperatures all hydrogen atoms are fully ionized. That is, each atom has lost its one and only electron. The remaining hydrogen ion (a positively charged proton) can not radiate light since it no longer has an electron capable of jumping between energy states. Instead, due to its extreme heat, a coronal loop emits copious amounts of extreme ultraviolet and x-ray radiation in addition to thermal emissions from its $100,000\text{ }^{\circ}\text{K}$ plasma. Coronal loop plasma also contains some heavy ions such as iron. These ions still have a complement of electrons left after ionization that can emit light at discrete wavelengths. These emission lines are frequently used to determine the temperature and density of coronal loop plasma.

The foot points of a coronal loop, anchoring it to the photosphere (Figure 12), typically move independent of each other. This is due to plasma flows in the Sun's underlying convection zone in addition to the Sun's differential rotation. As the foot points move, loop field lines become twisted and tangled until the loop eventually collapses. In extreme cases the energy built up in the tangled twisted field lines becomes so great that the field lines violently rupture creating a massive solar flare.

9.2.4 Coronal Helmet Streamers

A coronal helmet streamer, illustrated on the right in Figure 12, is a large coronal loop that has been pinched together into an elongated point at its top by slow speed solar winds emanating from regions around the coronal loop. With its pointed top, called a stalk, a helmet streamer resembles a 19th century German military helmet. Figure 13 is an image of helmet streamers taken during the 2017 total eclipse.



Figure 13 Coronal Helmet Streamers (source: space.com)

Helmet streamers usually overlie sunspots and prominences in the active streamer belt region of the Sun near the solar equator (Figure 14). A streamer is characterized by its bulb shaped base and elongated stalk extending outward from the top of the steamer. Two helmet streamers are shown in Figure 14 on the rim of the Sun. The warped heliospheric current sheet (Figure 15) runs through the middle of the streamer belt bisecting the belt and the two helmet streamers shown in Figure 14. The heliospheric current sheet is discussed in more detail in Section 14.2.8. Two pseudostreamers are also shown in the diagram, one in the upper right and the other in the lower left part of the diagram. These pseudostreamers exist outside the streamer belt and often appear during solar maximum when streamers ring the Sun. The significant difference between helmet and pseudostreamers is that pseudostreamers are located far from the heliospheric current sheet while the current sheet cuts through helmet streamers. Streamers are the Sun's outermost closed magnetic fields.

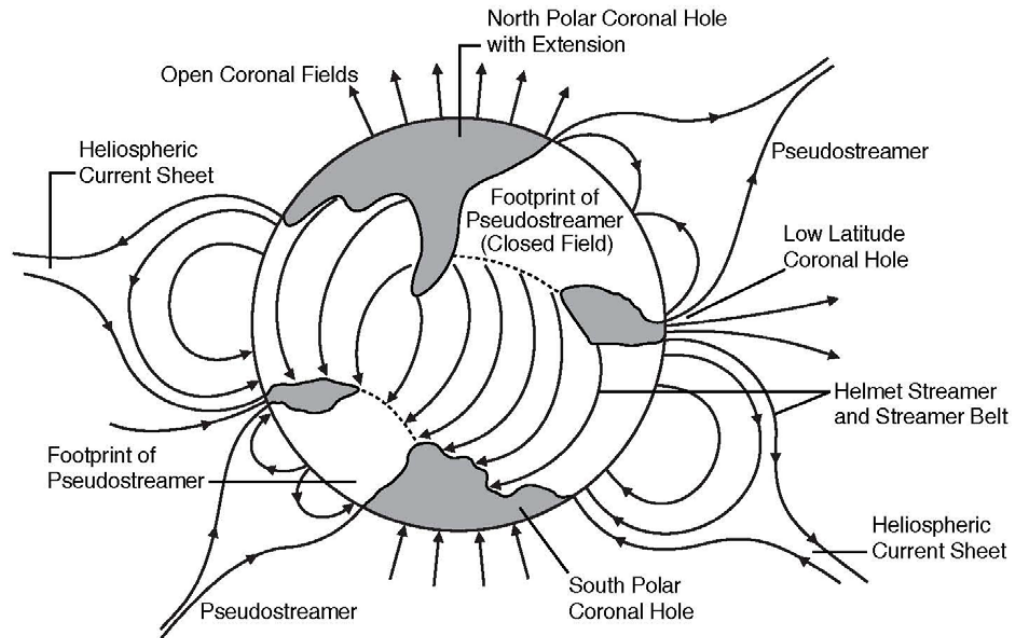


Figure 14 Structure of the Corona (source: Luhmann, Univ. of Calif. Berkeley)

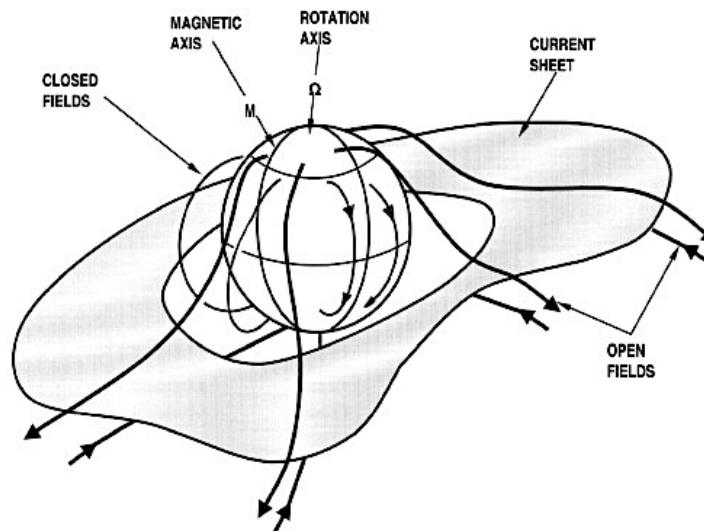


Figure 15 Solar Magnetic Field and Heliospheric Current Sheet (source: ScienceDirect.com)

Slow speed wind is the ambient background solar wind present throughout the solar cycle. This wind typically has a speed of 300 – 450 km/s and originates in the streamer belt region. The wind takes about 140 hours to traverse the distance between the Sun and Earth.

9.2.5 Coronal Holes

Coronal holes are dark areas seen in the solar corona when viewed in Extreme Ultra Violet (EUV) and soft X-ray light. They appear dark, like those shown in Figures 16, because they are cooler and less dense than the surrounding corona plasma.

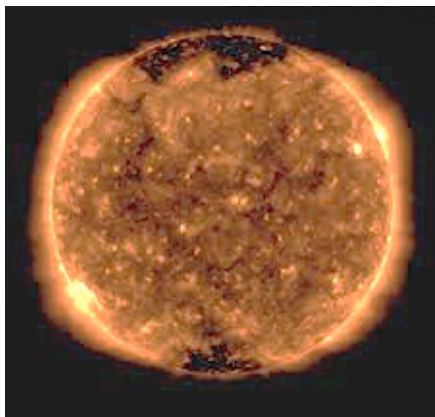


Figure 16 Large dark regions are coronal holes (credit: NOAA www.swpc.noaa.gov/phenomena)

Coronal holes can develop at any time and any location on the Sun. However, they occur most often at the solar north and south poles. Some of these grow and expand into lower solar latitudes, while others spin off individual holes. Coronal holes can also develop at regions other than the solar poles. Coronal holes occur most often and last longer during the declining phase of a solar cycle. In some cases coronal holes can last for several solar rotations (for several months).

Magnetic fields flowing out of coronal holes are open, expanding into interstellar space without returning to the Sun. These unipolar magnetic fields allow streams of relatively fast solar winds, known as high speed streams (HSS), to easily escape into space. In fact, long-lasting coronal holes are a major source of high speed streams that can buffet Earth for many days and then reoccur every 27 days as the Sun rotates.. Like the coronal holes from which they flow, high speed streams occur most frequently during the declining phase of the solar cycle.

9.2.6 Solar Flares

A solar flare is a massive, sudden, explosive releases of energy stored in the twisted tangled magnetic fields of coronal loops and to a lesser extent prominences (Figure 17). The amount of energy typically released by a large flare is equivalent to millions of 100 – megaton hydrogen bombs exploding all at once.



Figure 17 Solar flare (credit: wral.com)

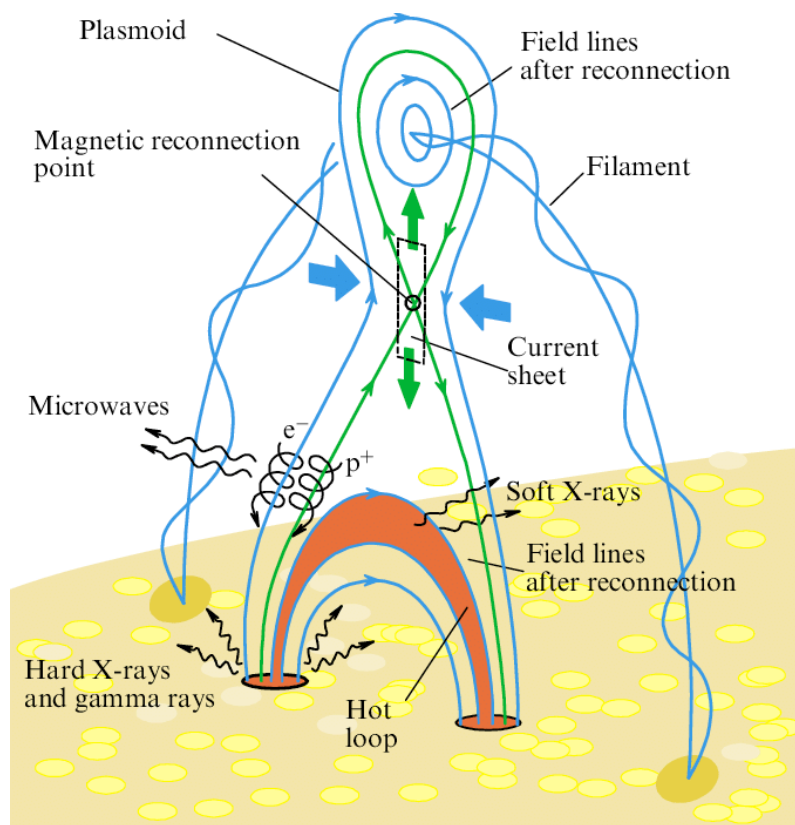


Figure 18 Formation of a solar flare (source: ResearchGate)

A flare occurs when the magnetic field lines of a coronal loop become stretched out, twisted, and tangled into an hour glass shape (Figure 18). In Figure 18 outbound field lines are marked by green arrows facing away from the Sun. Field lines returning to the Sun are marked by green arrows

pointing toward the Sun. Continued stretching and twisting squeeze outbound and returning magnetic field lines closer and closer together (in the neck of the hour glass) until the energy buildup becomes so great that outbound (+) and returning (-) magnetic field lines rupture forming a “short circuit” current sheet. Below the rupture the outbound and returning field lines reconnect into a much smaller hot magnetic loop anchored in the chromosphere as shown in Figure 18.

Hot plasma consisting of energetic electrons plus hydrogen and helium nuclei stream down the reconnected field lines. These energetic particles are traveling at nearly the speed of light. Intense heat is generated as they crash into the upper chromosphere. The intense heat and relativistic speed of the collisions cause sporadic nuclear reactions to occur within the chromosphere releasing a massive amount of energy in the form of gamma rays, x-rays, visible light, and radio waves.

Above the rupture, magnetic field lines also reconnect forming a plasmoid of hot electrons plus hydrogen and helium nuclei accelerated to energies exceeding 1 MeV. The plasmoid rapidly expands into interstellar space as a coronal mass ejection (CME) creating shock waves that propagate out far past Earth’s orbit in addition to producing high speed solar winds and solar energetic particles (SEPs).

A similar sequence of events can occur in a collapsing prominence but usually to a lesser extent.

9.2.7 Coronal Mass Ejections

A coronal mass ejection (CME) is a huge eruption of coronal plasma, with its associated frozen-in magnetic field, that moves outward from the Sun into interplanetary space. CMEs vary widely in size, shape, and speed. Some look like loops, other like bubbles, and some are irregular in shape. Figure 19 is an example of a CME.

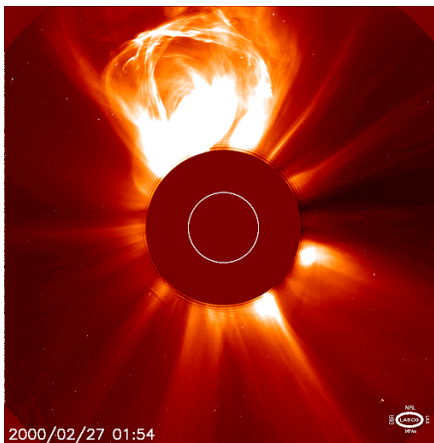


Figure 19 Coronal Mass Ejection (credit: www.astronet.ru)

CMEs are often caused by the collapse of coronal loops and prominences as magnetic fields re-align and reconnect into lower energy states. Catastrophic collapse of coronal loops and prominences can trigger solar flares which also produce CMEs.

A CME can eject billions of tons of coronal material outward from the Sun at speeds typically ranging from 200 to 500 km/s. Some energetic CMEs can reach speeds of 3,000 km/s or more. A shock wave is created when the CME travels faster than the background solar wind. The shock wave often accelerates charged particles ahead of it which can create intense particle (proton) radiation storms as the CME impacts Earth. During solar maximum several CMEs of various sizes and shapes occur per day. At solar minimum one CME is typically observed every 5 days or so.

Most CMEs are ejected outward from the Sun into the solar system away from the Earth. However, a CME launched in Earth's direction can arrive in as little as 15-18 hours. Slower CMEs may take several days to arrive. A CME expands as it travels away from the Sun. A large CME can encompass nearly a quarter of the distance between the Sun and Earth by the time it reaches Earth.

9.2.8 Solar Wind Sector Structure

One of the most significant aspects of the interplanetary magnetic field (IMF) is the abrupt changes in the polarity of the field's radial component near the ecliptic plane. The radial component B_x alternately switches from outward away from the Sun (+ direction) to inward toward the Sun (- direction) as the IMF sweeps past Earth. These changes often occur several times during the Sun's 27 days rotational period. The polarity reversals create a solar wind sector structure as view from the Earth. This structure is illustrated in Figure 20.

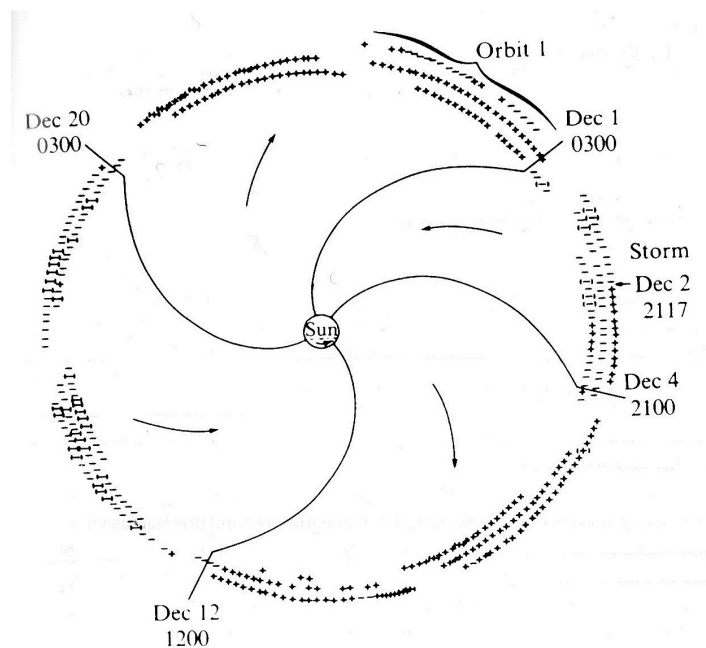


Figure 20 IMF Sector Structure (source: Hunsucker & Hargreaves)

Four sectors are shown in Figure 20. This is not always the case. The number of sectors typically vary from 2 to 4. In addition, the sectors are not necessarily the same size. In Figure 20 one of the sectors is smaller than the other three. In addition, the density and speed of the solar wind can

change from one sector to another. Density can vary by a factor of ten while the solar wind speed can change by a factor of 2.

The reason for the apparent sector structure is shown in Figure 21. On a large scale, the Sun's magnetic field is essentially bipolar with its magnetic poles M tilted with respect to its rotational axis Ω . Most of the magnetic field lines are closed in that they begin and terminate on the Sun's surface (they have two foot points on the Sun). The remaining magnetic field lines are open extending far out into interplanetary space without ever returning to the Sun. These magnetic field lines only have a single foot point on the Sun.

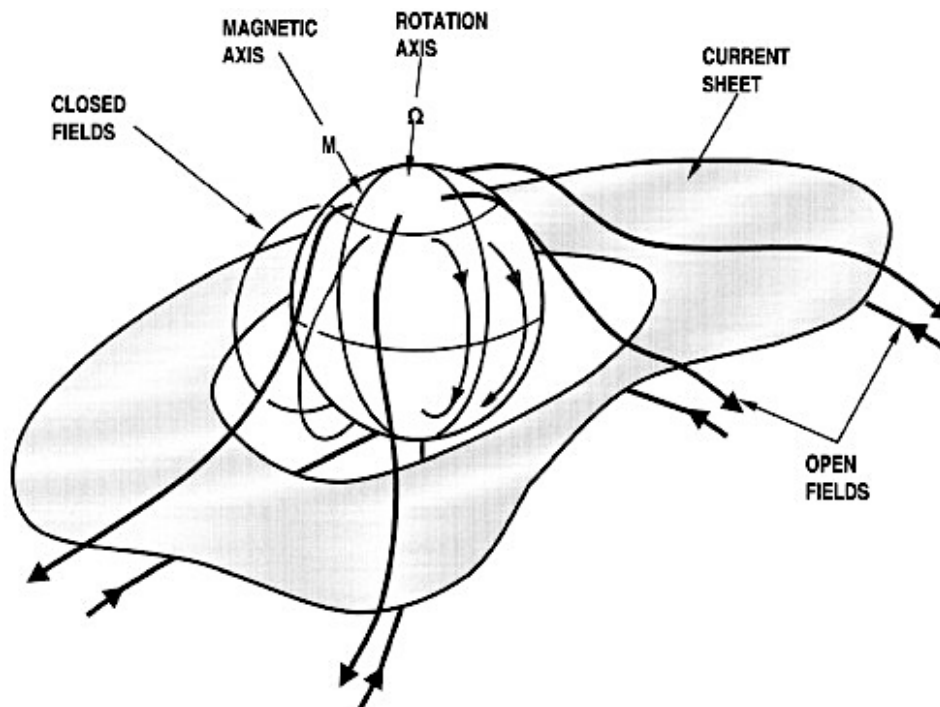


Figure 21 Solar Magnetic Field and Current Sheet (source: ScienceDirect.com)

The open magnetic field lines in the northern hemisphere of the Sun flow outward away from the Sun. These field lines are defined to be in a positive or in the + direction. In the southern hemisphere open field lines flow inward toward the Sun (in a negative or minus direction). Near the ecliptic plane the oppositely directed open field lines are separated by a thin current sheet known as the Heliospheric Current Sheet (HCS). Like the magnetic field itself, the current sheet is also tilted with respect to the Sun's rotational axis and ecliptic plane. Consequently, as the Sun rotates a spacecraft near the Earth could, for example, observe the outward magnetic field from the Sun's northern hemisphere. Later, as the tilted current sheet sweeps by, the spacecraft would see the magnetic field abruptly change direction to that of the Sun's southern hemisphere inward directed magnetic field. Consequently, to a spacecraft located on the ecliptic plane, the rotating magnetic field appears to have two sectors. A spacecraft situated high above the ecliptic plane and the titled

current sheet would see only a single sector, a continuous positive magnetic field flowing out from the Sun's northern hemisphere or a negative field flowing in toward the Sun's southern hemisphere.

Additional sectors may appear to an observer on the ecliptic plane, 4 sectors for example, because the current sheet is not flat but tends to be warped and undulate up and down creating folds much like the skirt of a pirouetting ballerina. For this reason, Figure 21 is known as the ballerina model. Figure 22 shows a three dimensional representation of the current sheet.

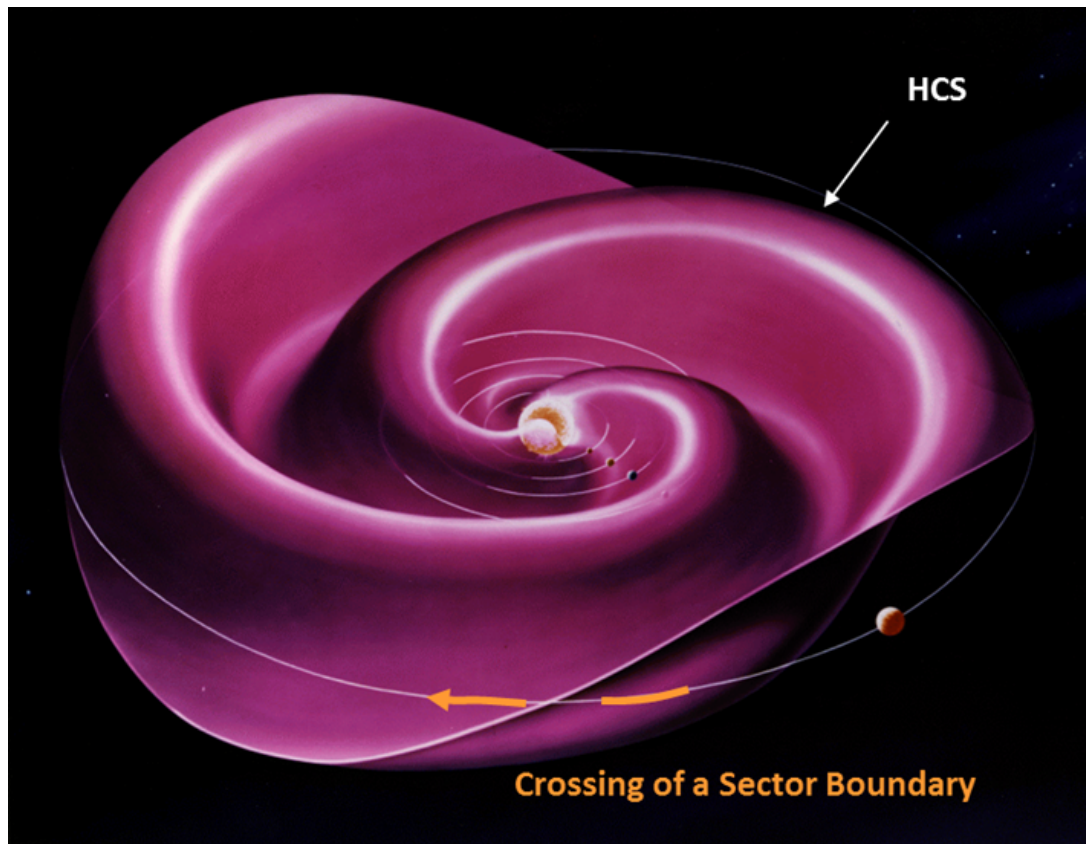


Figure 22 Three – Dimensional Representation of the Heliospheric Current Sheet
(source: Solar - Terrestrial Centre of Excellence)

A change in the solar wind radial (X_{GSM}) magnetic field orientation occurs when the Earth traverses a fold as illustrated in Figure 22. This is called a Sector Boundary Crossing (SBC). The change in orientation can be quite abrupt from outward (+ direction $\sim 180^\circ$) to inward (- direction $\sim 0^\circ$ relative to the X_{GSM} axis) or visa versa. The orientation angle is known as the phi angle. The phi angle is between 90° and 270° when the magnetic field is pointing outward away from the Sun. The angle is between 271° and 89° when the field is pointed inward.

A sector boundary crossing frequently causes variations in several solar wind parameters. In particular, the average magnetic field intensity can rise quickly, peaking about 1 day after the crossing, and then decay. The solar wind speed typically rises to a peak on days 1-2 and then it too

decays. In addition, the solar wind density often peaks around day one, falls to a minimum in the center of the sector, and then rises again toward the end of the sector. Finally, geomagnetic activity on Earth tends to increase on days 1-2 and then decays gradually through the rest of the sector.

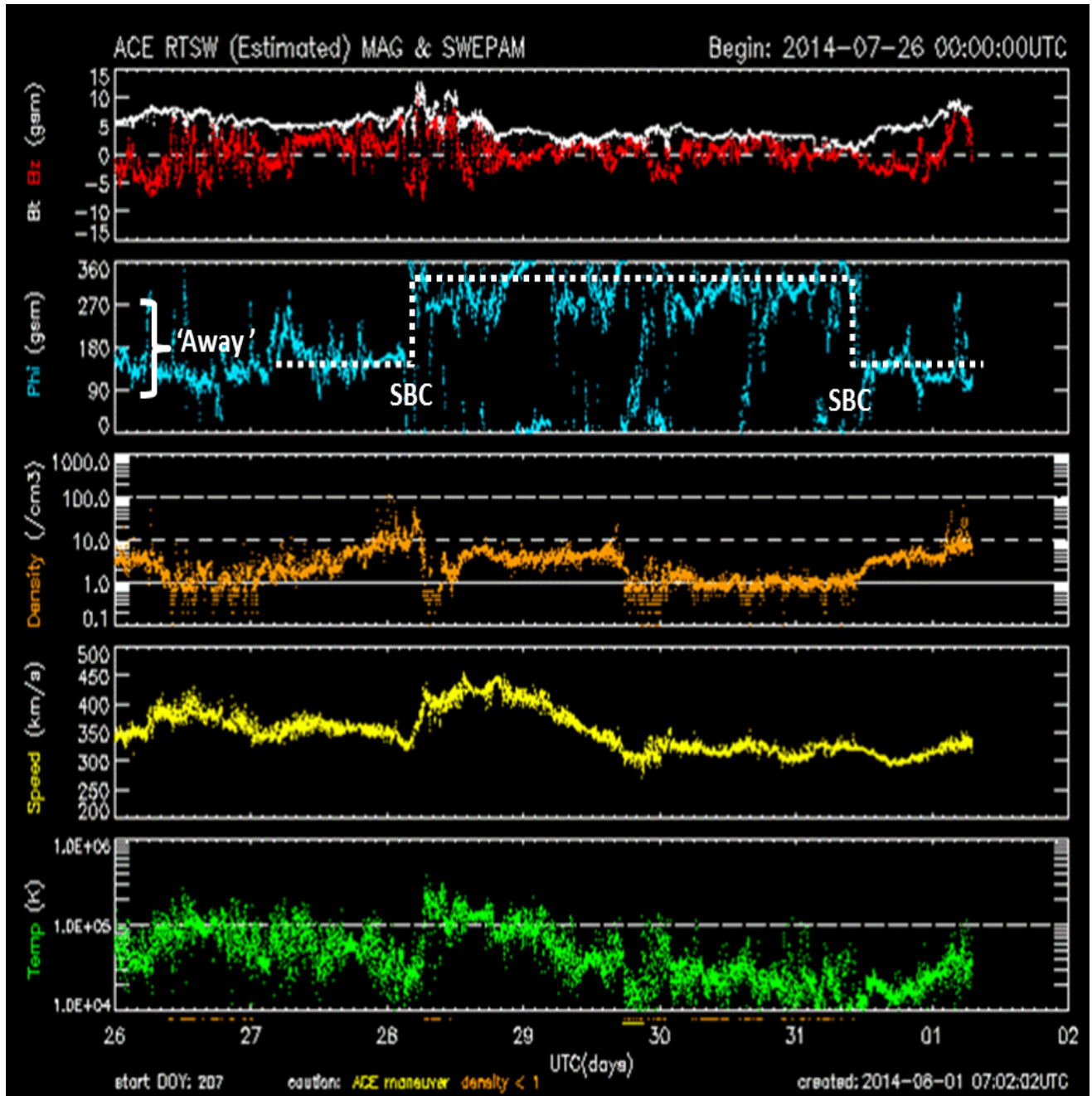


Figure 23 Solar Wind and IMF Parameters July 26 to August 1, 2015
(source: Solar - Terrestrial Centre of Excellence)

Figure 23 shows the solar wind parameters during a Sector Boundary Crossing occurring on July 28, 2014. Notice that the phi angle (blue trace) abruptly switches from outward away from the Sun ($\sim 180^\circ$) to inward ($\sim 360^\circ$). On July 31 the magnetic field abruptly switches back to outward.

However, only small changes, “blips” occur in the other solar wind parameters (temperature – green trace, speed – yellow trace, and density – orange trace) during the July 28th SBC. The changes are even less dramatic during the July 31st SBC. This is often the case. Large disturbances in the geomagnetic field are usually not associated with SBCs.

9.2.9 Corotating Interaction Regions (CIRs)

A Corotating Interaction Region (CIR) is formed by fast solar wind from a coronal hole overtaking slow ambient wind originating from near the coronal hole and in the streamer belt. The ambient wind on the left in Figure 24 is slowly rotating counterclockwise in a Parker-spiral. The fast wind, also rotating counterclockwise, is plowing through the ambient wind leaving a region of rarefied wind in its wake. A zone of compressed wind, a CIR, develops in front of the high speed wind as it crashes into the slower ambient wind. This phenomena is called corotating because the interaction region rotates along with the coronal hole on the Sun’s surface from which the high speed wind originates. Since coronal holes tend to be long-lived, often persisting for several months, high speed wind and the resulting CIRs sweep past the Earth at regular intervals corresponding to the 27 day solar rotation period.

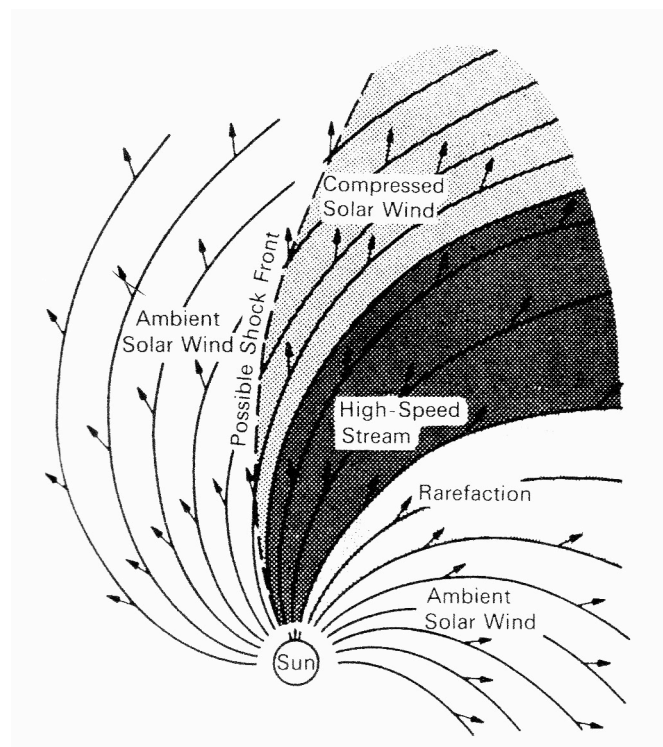
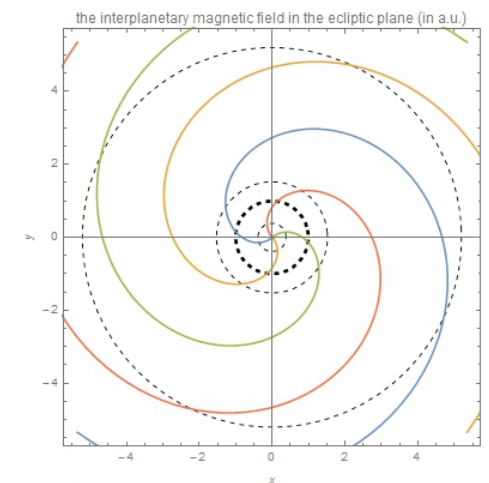


Figure 24 Corotating Interaction Region



Parker Spiral

The section of a corotating interaction region in the vicinity of Earth’s orbit is shown in more detail in Figure 25. In this figure the tan area is the CIR zone with the Sun located far below the lower edge of the picture. The unperturbed fast wind from a coronal hole is approaching the CIR from

below. Unperturbed slow wind is shown above the CIR. The high speed wind is slowed down, compressed and deflected to the right in the lower part of the CIR (indicated by the red arrow) as it collides with the slower wind ahead of it. The slow wind in turn is sped up, compressed and deflected to the left (red arrow) in the upper part of the CIR. The stream interface (the purple curved line) is the boundary between the fast and slow speed winds.

In Figure 25 the position of the Earth is represented by the green dashed line as the CIR rotates counterclockwise past Earth. Initially the Earth is in the unperturbed slow wind above (in this picture) the CIR. The Earth encounters the compressed slow wind first, followed by compressed fast wind, as the CIR rotates past Earth. After the CIR has passed, the Earth emerges into the unperturbed fast wind below the CIR. It takes about a day for the CIR to pass the Earth. The unperturbed fast wind is often referred to as a high speed stream (HSS).

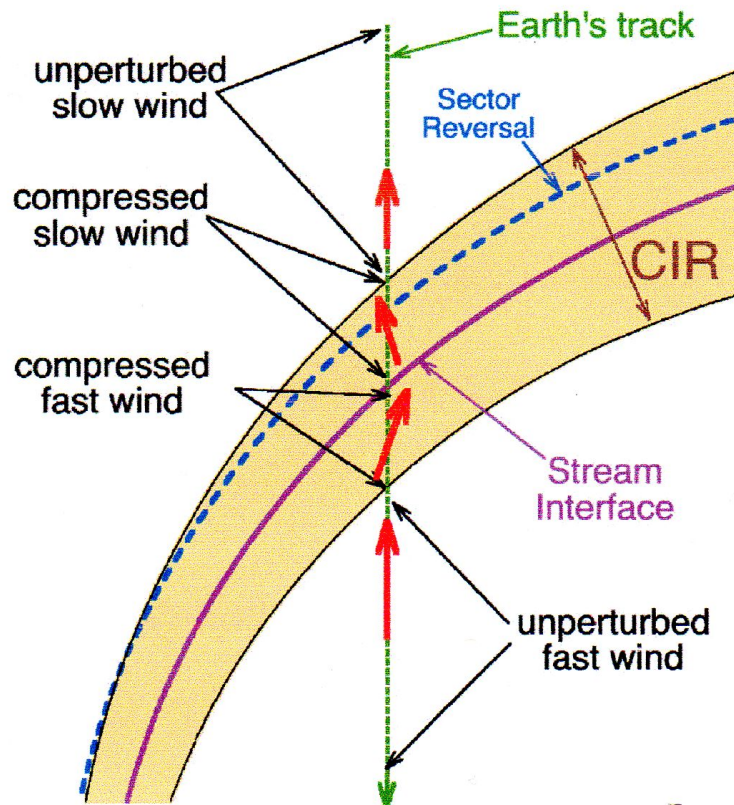


Figure 25 Detailed CIR Diagram (source J. Borovsky)

Compression within the CIR increases the number density n_{sw} of the solar wind plasma particles and its magnetic field strength B_{sw} . The elevated density and magnetic field increases the chance of a geomagnetic storm occurring. The CIR will quite likely induce a large storm if the enhanced magnetic field happens to be pointed southward. A northward directed magnetic field will usually

not produce a geomagnetic storm. While solar wind speed and density are factors, the orientation of the solar wind magnetic field has the greatest impact on the severity of a geomagnetic storm, or if a storm will occur at all.

The unperturbed slow speed wind is associated with either a helmet streamer, containing a sector reversal zone, or a pseudostreamer which does not have a sector reversal. As described above, a sector reversal occurs when the radial component of the solar wind magnetic field flips from inward toward the Sun to outward away from the Sun, or visa versa. If a sector reversal zone is present it tends to appear in the CIR a fraction of a day prior to passage of the stream interface. A sector reversal is shown as a blue dashed curved line in Figure 25. The sector reversal, in combination with increased slow speed wind density and magnetic field strength, often represents a calm before the occurrence of a large geomagnetic storm driven by the high speed wind. The calm often lasts for several days before the onset of the geomagnetic storm. The “calm before the storm” is generally not apparent when the slow speed wind originates from pseudostreamers since they do not have sector reversal zones.

9.2.10 Tilt of Earth’s Axis and Russell - McPherron Effect

The tilt of the Earth with respect to the Sun varies throughout the year resulting in spring, summer, fall, and winter. The Earth’s tilt, illustrated in Figure 26, also has an effect on the intensity of geomagnetic storms.

Figure 26a shows the tilt of the Earth at the March Equinox, June Solstice, September Equinox, and December Solstice. The red vector labeled $\vec{\Omega}$ is the Earth’s rotational axis. The Geocentric Solar Ecliptic (GSE) coordinate system is shown at point P. The radial X axis (X_{GSE}) is pointed to the Sun. The Y axis (Y_{GSE}) is tangent to Earth’s orbit in the ecliptic plane and perpendicular to the radial axis X_{GSE} . Finally, the Z axis (Z_{GSE}) is perpendicular to the ecliptic plane. Figures 26 b, c, and d shows the tilt of Earth’s rotational axis (red arrow) and magnetic axis (blue arrow) at significant times of the year.

The angle of Earth’s rotational axis relative to the Z_{GSE} axis is always 23.4° . The Earth’s axis gyrates around Z_{GSE} throughout the year as shown in Figures 26 b, c, and d. At the December Solstice Earth’s axis is pointed away from the Sun in the negative X_{GSE} direction. In June the Earth’s axis is pointed in the positive X_{GSE} direction toward the Sun creating long summer days in the northern hemisphere. The solstices are the only times of the year when the Y_{GSE} component of Earth’s tilt is zero. The June and December Solstices are shown in Figure 26c. During the March Equinox Earth’s axis is pointed in the positive Y_{GSE} direction, as shown in Figure 26d, while its X_{GSE} component is zero. During the September Equinox Earth’s axis is tilted in the negative Y_{GSE} direction, as shown in Figure 26b, again with a zero X_{GSE} component. At other times of the year (other than the equinoxes) the X_{GSE} component of Earth’s tilt is non-zero.

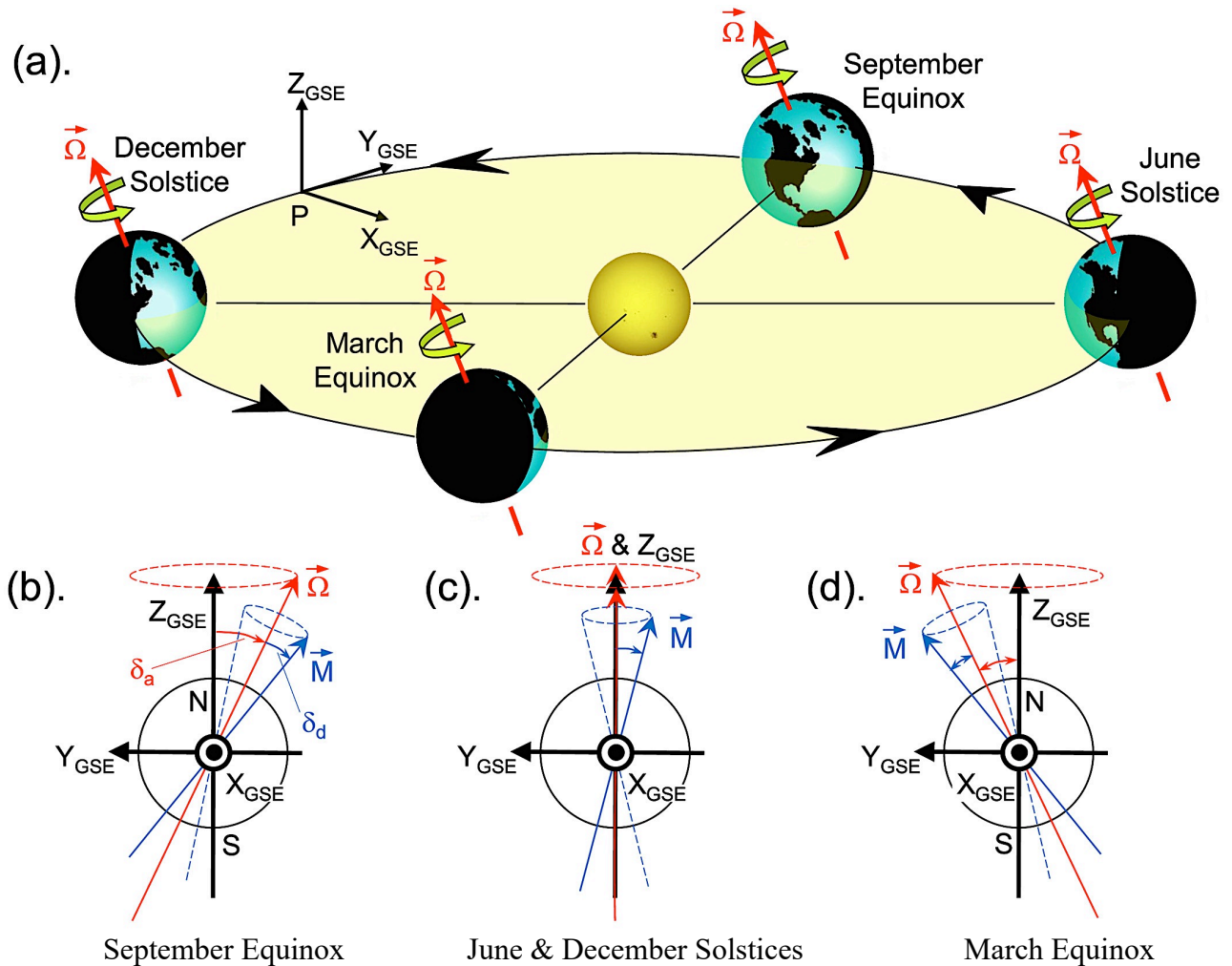


Figure 26 Tilt of the Earth during equinoxes and solstices (source: AGU Publications)

In spring and fall the Y_{GSE} tilt of Earth is such that Earth's magnetic field is more closely aligned with that of the unperturbed high speed winds. If the high speed wind magnetic field is directed southward (in the $-Z_{GSE}$ direction) it will connect with Earth's favorably aligned magnetic field creating geomagnetic storms that are more intense than at other times of the year. The unperturbed fast winds emanating from coronal holes can persist for several days or longer, so high speed wind driven geomagnetic storms can persist for a long time. However, few if any geomagnetic storms will occur if the high speed wind magnetic field happens to be directed northward. During the summer and winter Earth's tilt results in less favorable alignment with high speed wind magnetic fields resulting in less severe geomagnetic storms. These ideas were first suggested by Russell and McPherron in 1973.

9.2.11 IMF Clock Angle

In previous sections we have described geomagnetic storms as being the most intense when the solar wind's interplanetary magnetic field (IMF) is pointed southward. In more precise terms the direction of the IMF field is described as the IMF clock angle θ_{clock} defined with respect to the Geocentric Solar Magnetospheric (GSM) coordinate system shown in Figure 27.

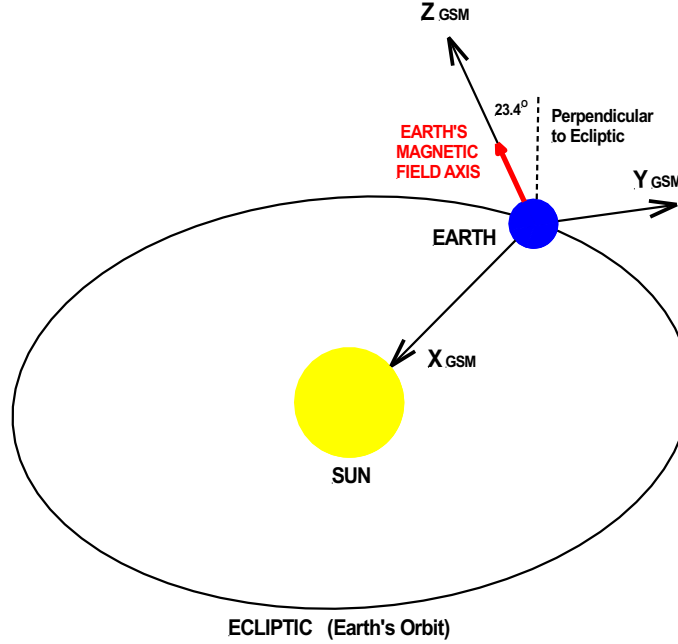


Figure 27 Geocentric Solar Magnetospheric (GSM) Coordinates (source: author)

The GSM coordinate system, centered on the Earth (geocentric), is defined relative to Earth's magnetic field axis. The radial x-axis (X_{GSM}) points from the center of the Earth to the center of the Sun. The z-axis (Z_{GSM}) is aligned with Earth's magnetic field axis and is the coordinate system north – south axis. The y-axis (Y_{GSM}) is perpendicular to both the x and z axis and is the dusk to dawn component.

The clock angle is defined as

$$\theta_{clock} = \cos^{-1} \left[\frac{B_z}{(B_y^2 + B_z^2)^{1/2}} \right]$$

where

B_z = the north – south component of the solar wind magnetic field vector \mathbf{B}

B_y = the dusk to dawn component of \mathbf{B}

The clock angle varies from 0° (purely northward IMF) to 180° (purely southward IMF). Thus, the intensity of a magnetic storm is greatest when the $\theta_{clock} = 180^\circ$ and least when $\theta_{clock} = 0^\circ$. The solar wind IMF field vector usually points in the Parker spiral direction at a $\theta_{clock} = 90^\circ$ which is in the ecliptic plane.

Most of the solar wind parameters (density, speed, magnetic field strength, etc.) vary slowly over a time period of hours to days. However, the direction of the IMF field, and thus the clock angle, vary much faster on a time scale of seconds and minutes. Thus, the intensity of a geomagnetic storm can change quickly.

9.3 Four Types of Solar Winds

There are four distinct types of solar winds originating from different regions of the Sun. They are:

1. Streamer belt wind,
2. Sector reversal wind,
3. Coronal Mass Ejection (CME) wind and
4. Coronal hole wind.

The origin of these winds, with the exception of CME wind, is shown in Figure 28. The average characteristics of the winds (including CME) are summarized in Table 1 and Figures 29.

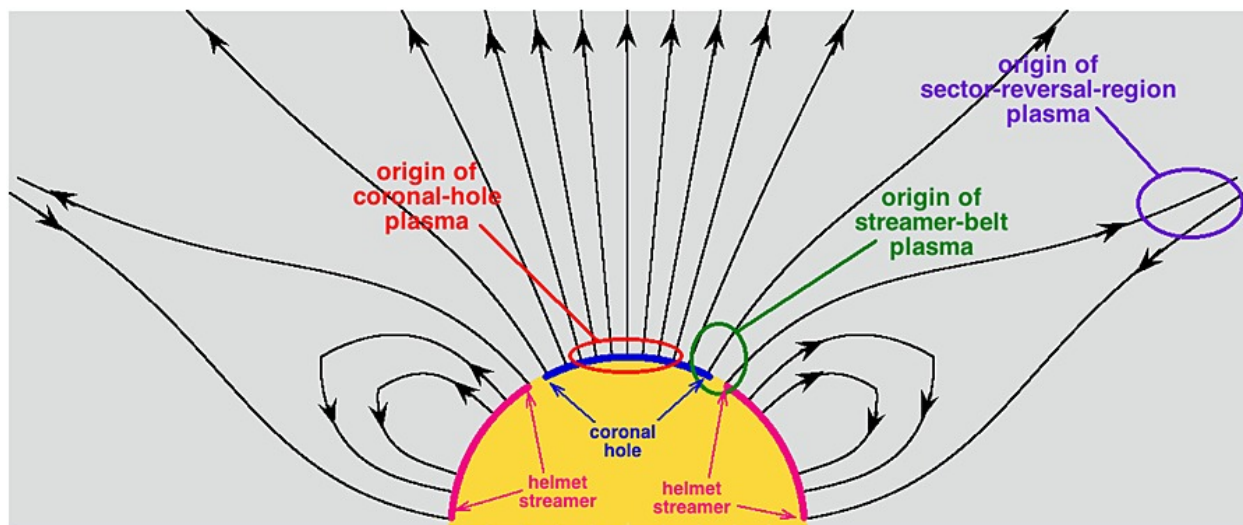


Figure 28 Source of Various Types of Solar Winds (source: Xu & Borovsky)

	Streamer Belt Wind	Sector Reversal Region Wind	CME (Ejecta) Wind	Coronal Hole Wind
Wind Speed	410 km/s	339 km/s	429 km/s	562 km/s
Number Density	5.6 particles/cm ³	10.7 particles/cm ³	6.4 particles/cm ³	3.2 particles/cm ³
Field Strength	5.3 nT	4.3 nT	10.6 nT	5.8 nT
Homogeneity	Quasi-homogeneous	Lumpy - plasma	Inhomogeneous	Quasi-homogeneous
Field Orientation	Parker spiral aligned	Non-Parker spiral aligned	Non-Parker spiral aligned	Parker spiral aligned
Hours to Earth	103 h	124 h	101 h	76 h
Occurrence Rate	41.6 %	23.9 %	11.5 %	23.9 %

Table 1 Summary of Solar Wind Characteristics (averages for the years 1995 – 2018)

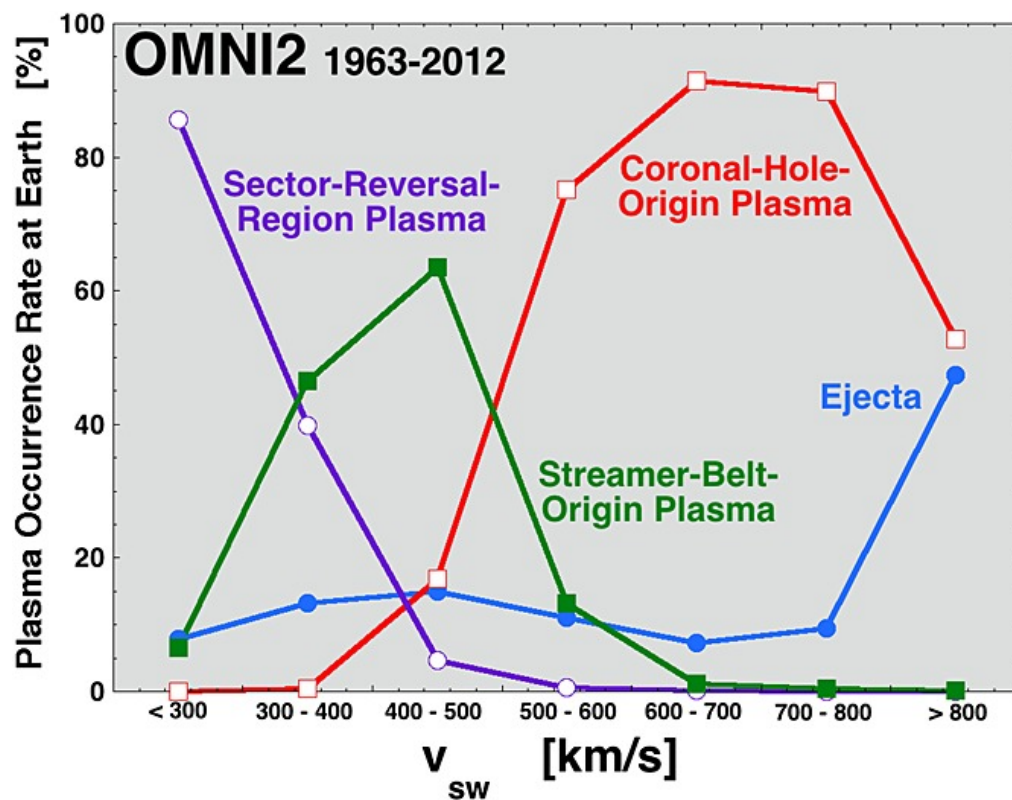


Figure 29 Solar Winds Speeds (source: Xu & Borovsky)

9.3.1 Streamer Belt Wind

Slow speed streamer belt wind is the ambient background solar wind that is continuously emanating from the Sun. For the years from 1995 through 2018 streamer belt wind accounted for 41.6 % of the solar winds reaching Earth. Interestingly, the 11 year solar cycle has little effect on streamer belt wind (Figure 30).

Streamer belt wind is believed to originate in the space between helmet streamers and from the edges of coronal holes, although their exact point of origin is still being investigated. Slow speed wind emanating from regions near coronal holes is particularly conducive to the formation of corotating interaction regions (CIR). Streamer belt wind is classified as slow solar wind with speeds typically ranging from 300 to 450 km/s (Table 1 and Figure 29). Streamer belt wind has the second lowest density of the four types of winds with a density of 5.6 particles per cm^3 . It also has the second lowest magnetic field strength at 5.3 nT. The magnetic field orientation of streamer belt wind tends to be Parker-spiral aligned with large fluctuations about the Parker-spiral direction. That is, the magnetic field points in the direction of the Parker-spiral shown in Figure 31 with a clock angle $\theta_{\text{clock}} = 90^\circ$. Streamer belt wind also tends to be somewhat homogeneous in its composition.

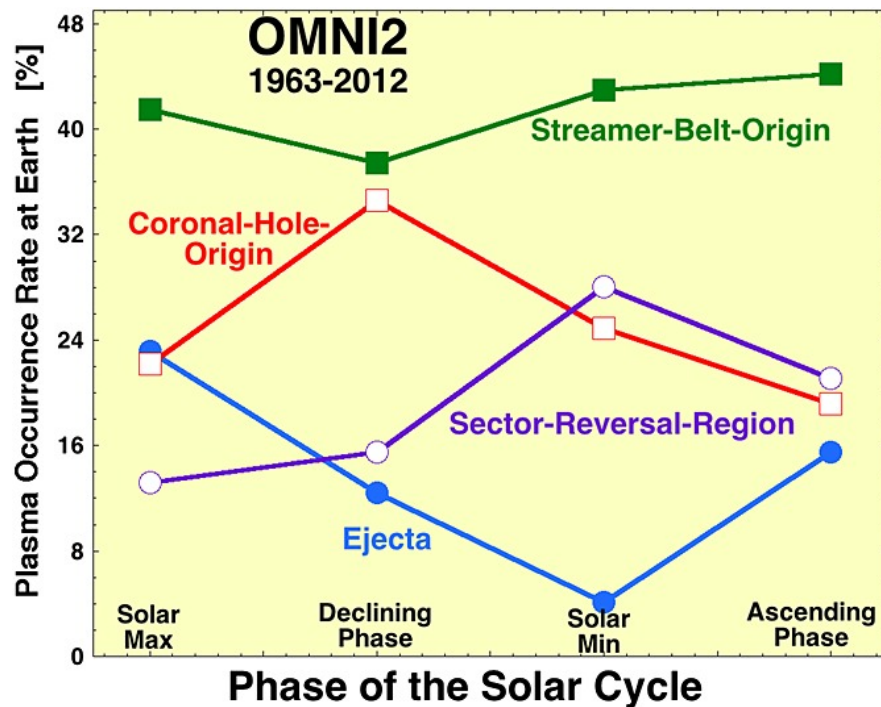


Figure 30 Occurrence of Solar Winds Throughout the solar cycle (source: Xu & Borovsky)

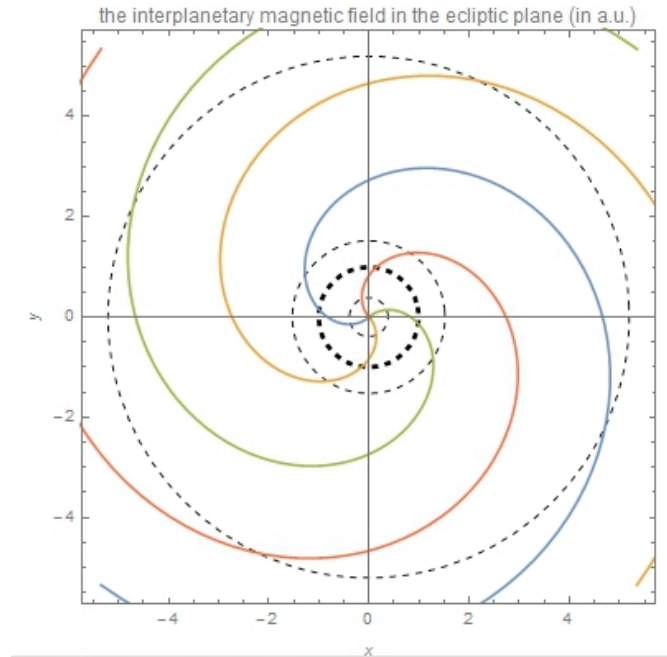


Figure 31 Parker spiral interplanetary magnetic field (source: Wolfram)

Figure 31 shows the direction of the interplanetary magnetic field (IMF) in the ecliptic plane as it spirals out from the Sun in the shape of a Parker-spiral. The dashed circles in Figure 31 are the orbits of selected planets. The inner most circuit is the orbit of Mercury while the heavy dashed circle is the orbit of Earth. The orbit beyond Earth is that of Mars. The orbit furthest from the Sun in Figure 31 is Jupiter. Notice that the direction of the IMF cuts across Earth's orbit at nearly a 45° angle. At Jupiter the direction of the IMF is almost in-line with Jupiter's orbit.

9.3.2 Sector Reversal Wind

A sector reversal wind is a blob of lumpy plasma originating from the stalk of a helmet streamer in the vicinity of the heliospheric current sheet. As shown in Figures 32 and 33, the current sheet bisects the streamer belt and helmet streamers located in the region. Pseudostreamers are located far from the heliospheric current sheet and thus do not produce sector reversal wind.

Sector reversal, along with coronal hole wind, are the second most common types of solar winds accounting for 23.9 % of the winds reaching Earth from 1995 to 2018. The speed of a sector reversal wind ranges from around 250 to 400 km/s (Table 1 and Figure 29). Consequently, it is classified as very slow solar wind. Sector reversal wind is the most dense of the four types of winds with a density of 10.7 particles per cm^3 . However, it has the weakest magnetic field strength at 4.3 nT. Sector reversal wind is non-homogeneous with large sudden changes in density, temperature, and magnetic field strength. In addition, the magnetic field orientation of sector reversal wind does not tend to be Parker-spiral aligned.

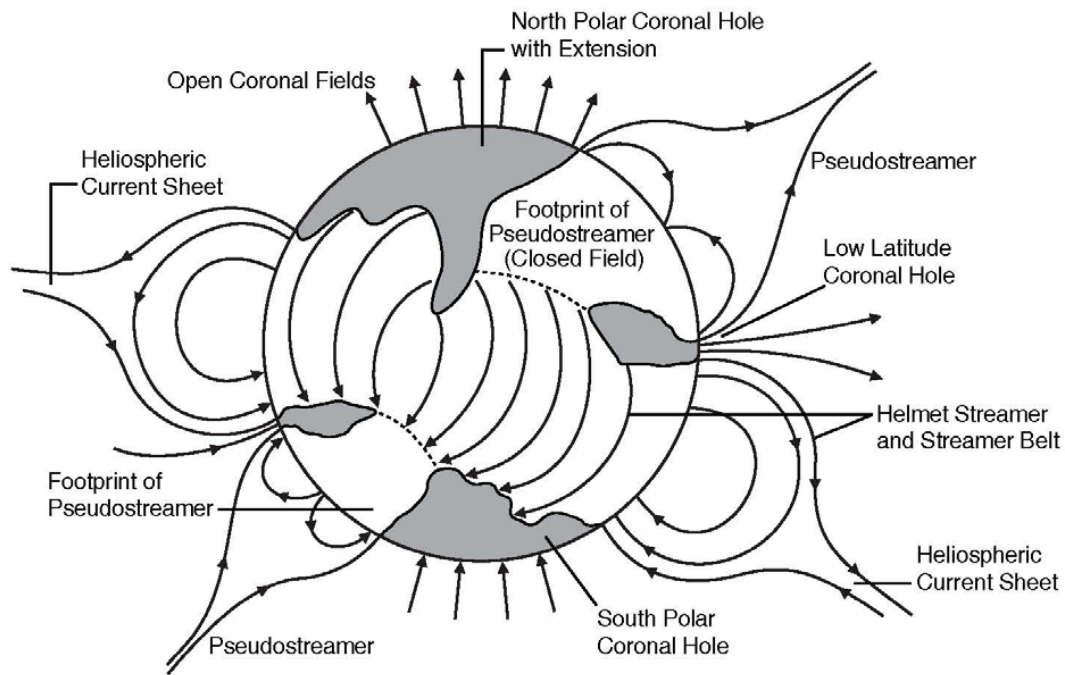


Figure 32 Structure of the Corona (source: Luhmann, Univ. of Calif. Berkeley)

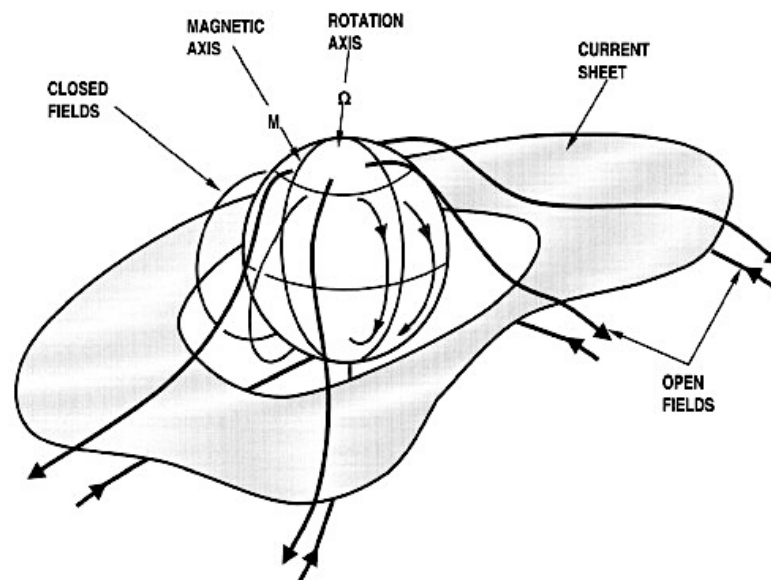


Figure 33 Solar Magnetic Field and Heliospheric Current Sheet (source: ScienceDirect.com)

Solar winds consist primarily of very slow sector reversal wind and slow streamer belt wind during solar minimum. These slow speed winds account in part for the low occurrence of geomagnetic

storms and substorms during solar minimum. Typically, one substorm occurs about every 2 or 3 days during solar minimum. In contrast substorms occur at a rate of about 4 per day during the declining phase of the solar cycle when coronal hole wind is most prevalent.

9.3.3 Coronal Mass Ejections (CMEs) Wind

Coronal mass ejections accounted for 11.5 % of the solar winds reaching Earth from 1995 to 2018.

CME wind has the strongest magnetic field strength at 10.6 nT, the second highest speed, and second highest density of the four types of wind. CME wind is non-homogeneous with large sudden changes in density, temperature, and magnetic field strength. In addition, its magnetic field orientation is not Parker-spiral aligned. With the strongest magnetic field and second highest density and speed, coronal mass ejection winds have the potential for producing strong geomagnetic storms.

Coronal mass ejections are rarely seen during solar minimum. However, they frequently occur around solar maximum becoming the major cause of solar maximum geomagnetic storms. As illustrated in Figure 30, the rate of CMEs steadily decreases during the declining phase of the solar cycle, but then increase in frequency during the ascending phase of the next cycle. During solar maximum several CMEs occur per day. At solar minimum one CME is typically observed every 5 days or so.

9.3.4 Coronal Hole Wind

Coronal hole and sector reversal winds are the second most common type of solar winds reaching Earth, each occurring 23.9 % of the time from 1995 to 2018. Streamer belt wind is the most common.

Coronal hole wind is classified as fast solar wind with speeds of 500 to over 750 km/s (over 1 million miles per hour). Coronal hole wind has the lowest density of the four types of winds with a density of only 3.2 particles per cm^3 , but the second highest magnetic field strength at 5.8 nT. The magnetic field orientation of coronal hole wind tends to be Parker-spiral aligned with large fluctuations about the Parker-spiral direction. In addition, coronal hole wind tends to be somewhat homogeneous in its composition.

Intervals of fast wind from coronal holes are referred to as high speed streams (HSS).

Coronal hole wind occurs most frequently during the declining phase of the 11 year solar cycle, as shown in Figure 30. Approximately 34% of the solar winds arriving at Earth during the declining phase come from coronal holes.

High speed streams originating in coronal holes are a major cause of geomagnetic storms and substorms during the solar cycle declining phase, due to their high speed, second strongest magnetic fields, and tendency to produce density enhancing corotating interaction regions (CIR).

9.4 Geomagnetic Storms

There are two types of geomagnetic storms:

1. Coronal hole - CIR induced storms, and
2. CME storms.

9.4.1 Coronal hole - CIR storms

As described earlier, a Corotating Interaction Region (CIR) is formed by fast solar wind from a coronal hole overtaking slow ambient wind. The ambient wind on the left in Figure 34 is slowly rotating counterclockwise in a Parker-spiral. The fast wind, also rotating counterclockwise, plows through the ambient wind leaving a region of rarefied wind in its wake. A zone of compressed wind, with an increased plasma density and magnetic field strength, develops in front of the high speed wind as it collides with the slower moving ambient wind (Figure 35). The compression zone typically takes about a day to pass Earth with several days of fast wind following.

This phenomena is called corotating because the interaction region rotates along with the coronal hole on the Sun from which the high speed wind originates. Since coronal holes tend to be long-lived, often persisting for several months, high speed winds and the resulting CIRs typically sweep past the Earth at regular intervals corresponding to the 27 day solar rotation period.

The magnetic field within the solar wind CIR compression and high speed wind that follows are parker spiral oriented with a clock angle of roughly 90° . However, the Russell-McPherron effect can come into play to produce southward clock angles ($\theta_{clock} \approx 180^\circ$). Hence, coronal hole - CIR induced geomagnetic storms tend to occur during the spring and fall and to a much lesser extent in summer and winter. Coronal hole - CIR storms also tend to repeat every 27 days as long as the high speed stream emanating from a coronal hole persists.

As described above, a sector reversal occurs when the radial component of the solar wind magnetic field flips from inward toward the Sun to outward away from the Sun, or visa versa. The presence of a sector reversal in combination with increased slow speed wind density and magnetic field strength often represents a calm before the occurrence of a large scale coronal hole - CIR storm. The calm often lasts for several days before the onset of the storm. The “calm before the storm” is not present when the slow speed wind originates from pseudostreamers since they do not have sector reversal zones.

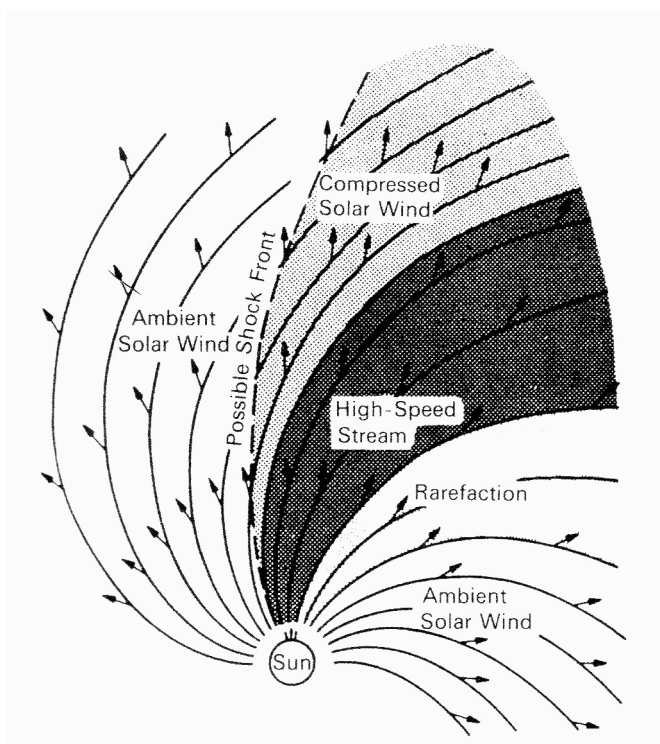


Figure 34 Corotating Interactive Region (source: Hunsucker & Hargreaves)

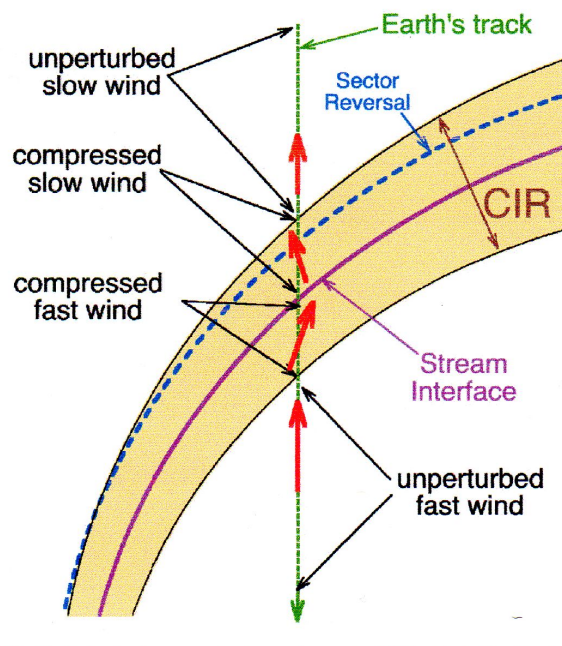


Figure 35 Detailed CIR Diagram (source J. Borovsky)

9.4.2 Coronal Mass Ejection Storms

A CME is a short duration eruption, an outward burst of plasma, from the Sun's corona typically caused by the collapse of coronal loops and prominences as magnetic fields re-align and reconnect into lower energy states. Catastrophic collapse of coronal loops and prominences can trigger solar flares. Solar flares also produce CMEs.

A short CME burst can eject billions of tons of coronal material outward from the Sun at speeds typically ranging from 200 to over 700 km/s. If the speed of the CME plasma is great enough (> 500 km/s) its collision with an ambient stream of slow wind ahead of it can produce an interplanetary shock wave that travels outward far past Earth's orbit. Impact of the CME plasma with the slow speed wind compresses and accelerates the wind, greatly increasing the wind's density and strength of its magnetic field. Whether or not the intensified wind creates a geomagnetic storm upon reaching Earth's magnetosphere depends on the orientation of the wind's magnetic field. An intense magnetic storm can be expected if the magnetic field is oriented southward.

The onset of a CME storm typically occurs when the interplanetary shock passes the Earth, followed by arrival of dense high speed solar wind that drives the magnetosphere bow shock closer to the Earth, compressing the magnetosheath in the process. The D_{st} index, which is a measure of the equatorial ring current strength, is sensitive to the ram pressure of solar wind impacting the magnetosphere. As the shock passes a positive jump occurs in the D_{st} index (Figure 36). The positive jump is known as the storm sudden commencement (SSC).

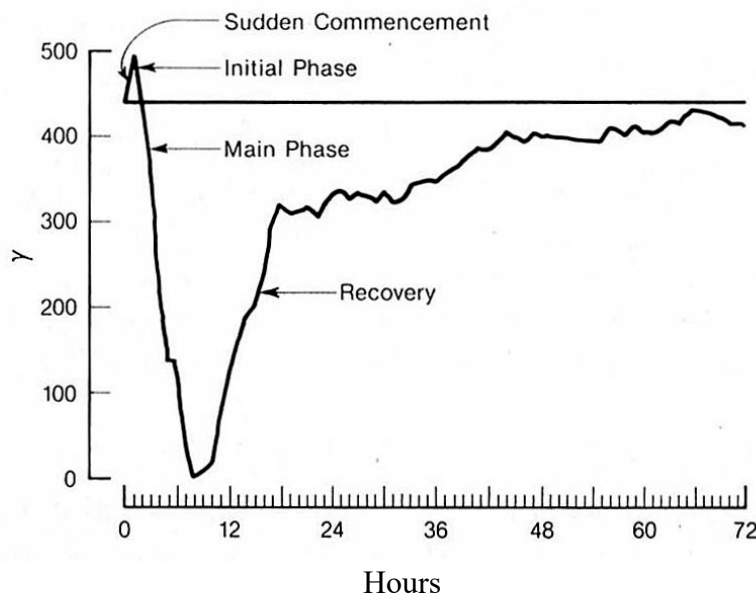


Figure 36 D_{st} Index: Phases of a Magnetic Storm (source: Davies)

During solar maximum several CMEs of various sizes and shapes occur per day. At solar minimum one CME is typically observed every 5 days or so.

9.4.3 Differences Between CME and Coronal Hole - CIR Storms

CME and CIR geomagnetic storms have distinctly different characteristics, including:

- CME storms typically last a day or so (a short one time burst) while CIR storms often last several days and can repeat every 27 days.
- CME storms are most prevalent during solar cycle maximum. CIR storms occur most often in the spring and fall during the declining phase of the solar cycle.
- CME storms often begin with a storm sudden commencement while CIR storms generally do not.
- CME storms are generally associated with very strong ring currents (large $-D_{st}$ values), formation of new radiation belts, intense aurora, and geomagnetically induced electrical currents. CIR storms are associated with high energization of the outer electron radiation belt and high levels of spacecraft charging
- CIR storms are often preceded by a “calm before the storm” while CME storms are not.

9.5 Geomagnetic Auroral Substorms

The magnetic storms described so far are observed and measured primarily at mid and low latitudes. These global geomagnetic storms typically last up to several days. Other short duration storms occur within the polar regions (at high geomagnetic latitudes). These storms are associated with the northern and southern auroral light displays (Figure 37) and thus are called auroral substorms. A substorm may last an hour or so, disappear, and then reoccur a couple of hours later.

A major geomagnetic storm usually has associated with it a number of auroral substorms. However, the reverse is not true. Substorms may appear on their own when there are no mid or low latitude storms.

The occurrence of auroral substorms vary with the solar cycle, seasonally, diurnally, and with solar rotation. The solar cycle and seasonal variations are similar to as those for geomagnetic storms. Auroral activity, like that of geomagnetic storms, is greatest following solar maximum. Seasonally, the greatest number of substorms occur during the spring and fall equinoxes. In addition, auroral activity varies throughout the day with the greatest auroral activity occurring near local midnight.

Finally, the Sun's rotational period can cause auroras to reappear every 27 days when long term active regions persist on the Sun.



Figure 37 Auroral Display (source: sciencephoto.net)

A substorm develops when energetic solar wind particles gain entry into the magnetosphere and spiral down magnetic field lines into the polar region in a rough circular area called the auroral oval illustrated in Figure 38.

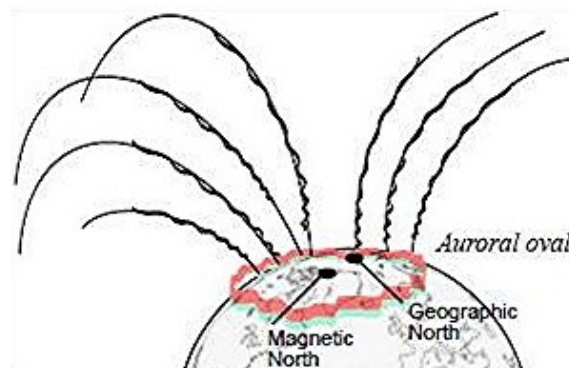


Figure 38 Formation of Auroral Oval (source: NOAA Space Environment Center)

There are two mechanisms by which this occurs. They are called:

1. The directly driven process, and
2. The loading – unloading process.

A directly driven substorm typically lasts about two hours. It occurs as arriving high energy solar wind particles find their way into the cusp zone and travel down unobstructed into the polar region. These particles could come from the solar wind generating an ongoing coronal – CIR or CME geomagnetic storm. They could also be associated with a solar wind without the strength or orientation to produce a full geomagnetic storm.

The second type of substorm consists of a loading and unloading process and is typically only 10 to 20 minutes in duration. In this case charged particles build up midway down the magnetotail (loading), become energized by strong passing IMF fields, and then propelled (unloading) down magnetic field lines into the polar region.

Beautiful shimmering auroral light displays, like that shown in Figure 37, are the visual aspect of auroral substorms. They occur in both the northern and southern polar regions where they are known as aurora borealis in the north and aurora australis in the southern hemisphere.

Aurora displays frequently include magnificent curtains of light, rays, and arcs that extend across the sky from horizon to horizon. They often appear to pulsate and dance under the influence of ionospheric winds. No two auroral displays are alike. Instead, they vary considerably in shape and brightness over time intervals from seconds to minutes. The patterns and shapes of the aurora are determined by the changing flow of incoming charged particles and varying magnetic fields.

Visual auroras are formed as high energy incoming particles, primarily electrons, collide with neutral atoms and molecules in Earth's upper atmosphere, exciting them to higher energy levels. Atoms and molecules typically remain in an excited state for about a second or two before dropping back to their normal unexcited state, dissipating photons of energy in the process. The dissipated photons produce the auroral displays. The color of an aurora depends on the specific atmospheric gas involved and the energy of the colliding particles. Most auroral features are greenish yellow produced by excited oxygen atoms. High altitude oxygen atoms emit a reddish light as do excited nitrogen molecules at low altitudes, giving the tops and bottoms of tall curtains their reddish color. Figure 39 illustrates the source and altitudes at which the various aurora colors occur.

The vast majority of aurora displays form in the E region of the ionosphere from about 90 to 130 km above Earth's surface. However, aurora can extend down to around 70 km and up to nearly 600 km, as shown in Figure 40a. The height of various aurora displays, measured from their lower edge, is shown in Figure 40b. Most of the bright displays are less than 20 km tall and generally very thin ~ 100 m thick.

An auroral display usually begins as one or more arcs in the auroral oval brighten. As they brighten auroral formations start appearing within the arcs. After 30 minutes to an hour the formations fade and disappear marking the end of the substorm. The sequence is likely to repeat 2 to 3 hours later.

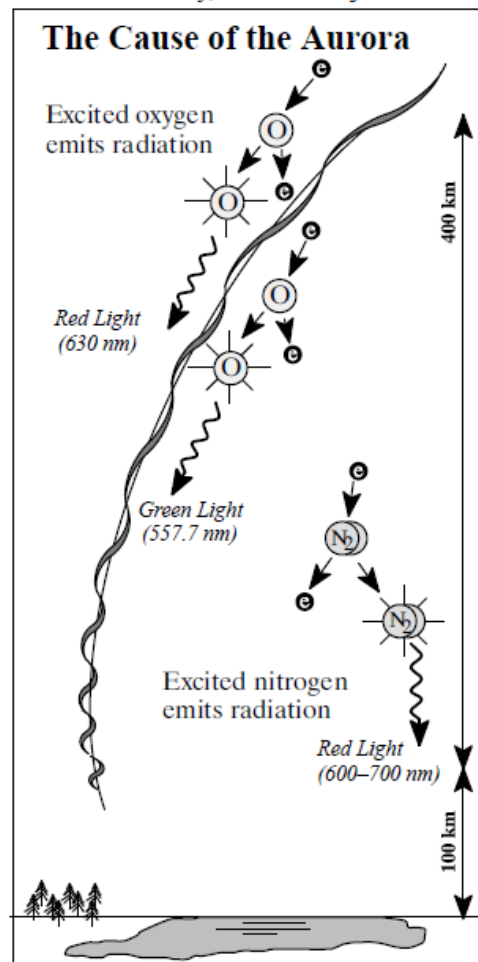


Figure 39 Colors of Auroral Displays (source: NOAA Space Environment Center)

In addition to discrete aurora (curtains, arches, rays, etc.) there are also diffused aurora, or auroral glow, such as that shown in Figure 41. Diffused aurora are more difficult to see from the ground because of their lower light intensity, although they produce as much total light as discrete aurora. Satellite images of the aurora tend to be dominated by the diffuse aurora. Discrete forms appear in these images both within the diffuse area and poleward of it. However, discrete forms are seldom seen on the equatorial side of a diffuse aurora. The charged particles forming the discrete and diffused aurora are believed to originate from different sources.

Atmospheric atoms and molecules can also be ionized by incoming high energy particles as well as being excited to higher energy levels. Ionization occurs if the kinetic energy of an incoming particle is high enough to knock an electron out of an atom or molecule. When this occurs the atom or molecule becomes an ion, having a net positive charge instead of being electrically neutral. The

ejected electron becomes a free unattached electron with a single negative charge traveling on its own in the vicinity of the collision.

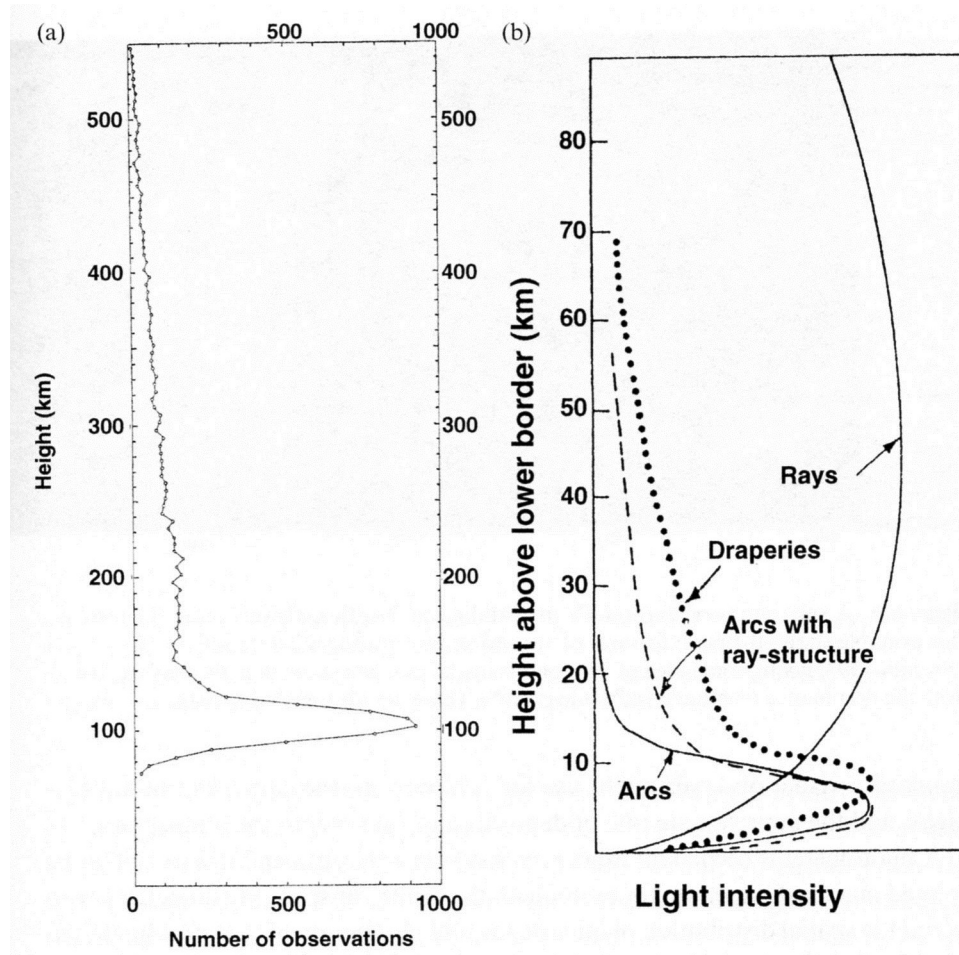


Figure 40 Height of Auroral Displays (source: Hunsucker)

Ionization increases E region electron density and conductivity permitting an intense electrical current, known as an auroral electrojet, to flow in the polar E region. The electrojet disrupts the geomagnetic field in the auroral zone causing it to vary violently in synchronism with the visual auroral display. The electrojet is thus responsible for the magnetic aspects of an auroral substorm while excited atoms and molecules are responsible for the visual part of the storm.

During quiet geomagnetic conditions an auroral oval is around 3,000 km in diameter centered over a magnetic pole. In general, the ovals are located between 64 to 70 degrees latitude in both north and south hemispheres. An oval is at its lowest latitude at midnight and highest latitude around noon. The width of an oval also varies. It is greatest at midnight, about 10° wide in latitude, and narrowest at noon.



Figure 41 Diffuse Aurora (source: NASA ISS)

Images from space confirm that the oval is a permanent ring of light around a magnetic pole, though the intensity of the light varies considerably from one area of the ring to another. There can also be considerable difference between the night and day sectors of an oval. The night sector may be more active than the day sector, or visa versa. During geomagnetic storms the ovals grow brighter and larger allowing them to be observed at lower latitudes, for example in the northern United States and central Europe. For very large storms the aurora can sometimes be seen as far south as Washington D.C. and Virginia.

It is important to note that the oval is fixed with respect to the Sun with the Earth rotating beneath it.

The auroral oval is actually two ovals, an inner and an outer oval.

The inner oval is the visual or luminous oval. Its characteristics include:

- Luminosity,
- Sporadic – E ionized patches
- Spread – F zones, and
- Soft X-ray emissions.

The outer oval is nearly circular. It is situated lower in latitude at approximately 60° to 70° magnetic. The characteristics of the outer oval include:

- Diffuse aurora,
- Radio wave absorption,
- Sporadic – E at an altitude of 80 to 90 km, and
- Slow fading of VHF scatter signals.

Activity in the outer oval is greatest during the day. In contrast, the highest level of inner oval activity occurs at night. Both ovals occupy about the same latitude at midnight but become increasingly separated toward noon. In addition, they both exhibit substorm activity.

High energy particles responsible for the outer oval are thought to originate in the Van Allen radiation belts, and have higher energy levels than those forming the inner oval. Inner oval high energy particles are believed to originate in the magnetic tail.

The OVATION Aurora Forecast Model, Figure 42, predicts the intensity and location of the aurora for the time shown at the top of the map. This probability forecast is based on current solar wind conditions measured at the L1 point in space, assuming a 30-minute delay time between L1 and Earth. L1 is a location in space where the gravitational forces of the Earth and Sun are equal creating a point of equilibrium where spacecraft may be "parked" to observe the Sun and solar wind conditions.

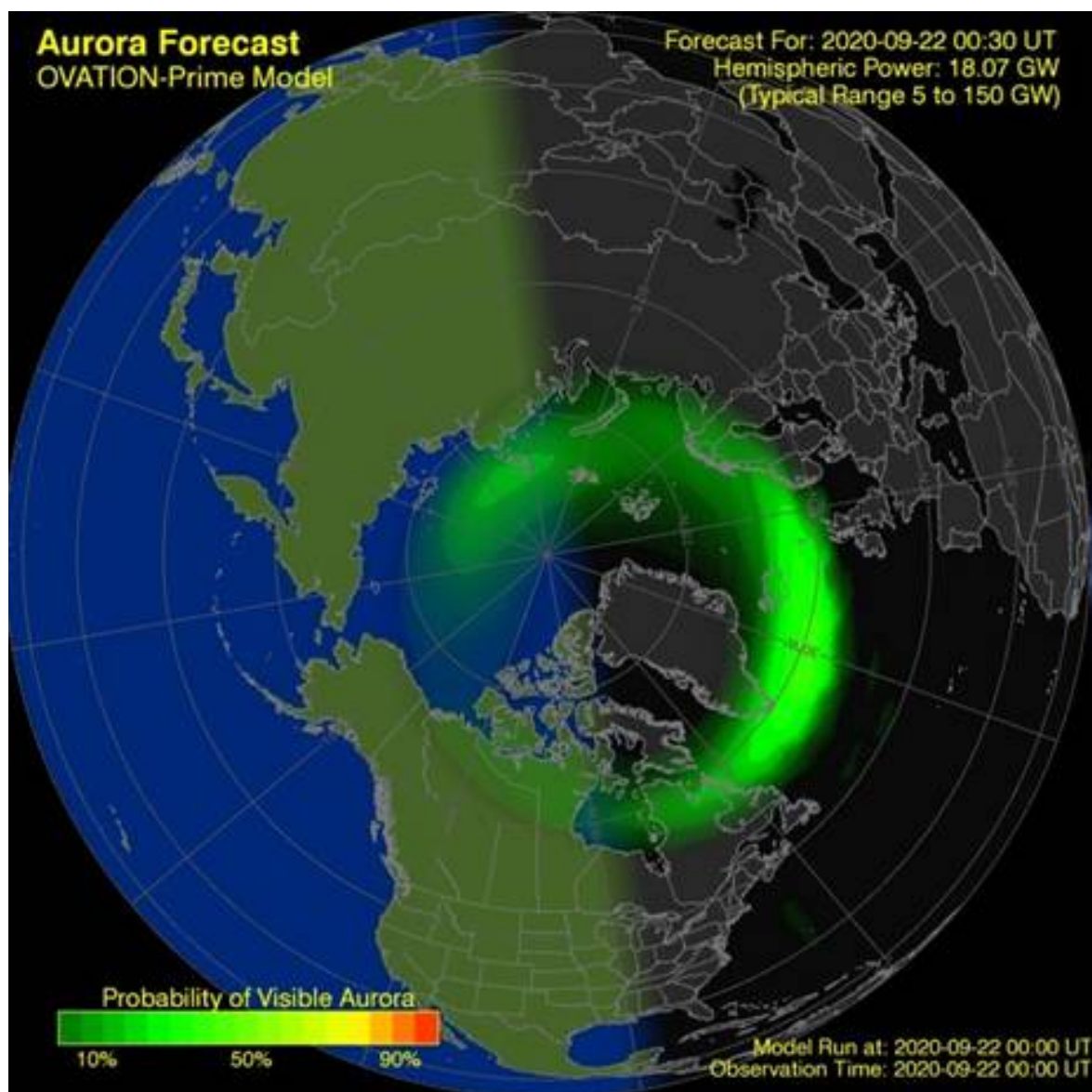


Figure 42 Auroral Oval September 22, 2020

A 30-minute delay corresponds approximately to an 800 km/s solar wind speed as might be encountered during geomagnetic storm conditions. In reality, delay times vary from less than 30 minutes to an hour or so.

In Figure 42 the sunlit side of Earth is indicated by the lighter blue of the ocean and the lighter color of the continents. The day-night line, or terminator, is shown as a region that goes from light to dark. The lighter edge marks the zone where the Sun is just at the horizon. At the darker edge the Sun is 12 degrees below the horizon. The aurora is not visible during daylight hours, however, the aurora can often be observed about an hour before sunrise or just after sunset.

The current aurora forecast can be viewed by clicking on “Aurora” under “Current Conditions” on the www.skywave-radio.org website.

The auroral oval marks the division between closed and open magnetic field lines illustrated in Figure 43. Both ends of closed magnetic field lines connect back to Earth. Open field lines on the other hand are connected to Earth at only one end. The other end extends out into space.

The region poleward of the oval is generally accepted to be the polar cap. Magnetic field lines within the polar cap are open, meaning that they flow outward from the polar region and connect with the solar wind Interplanetary Magnetic Field (IWF).

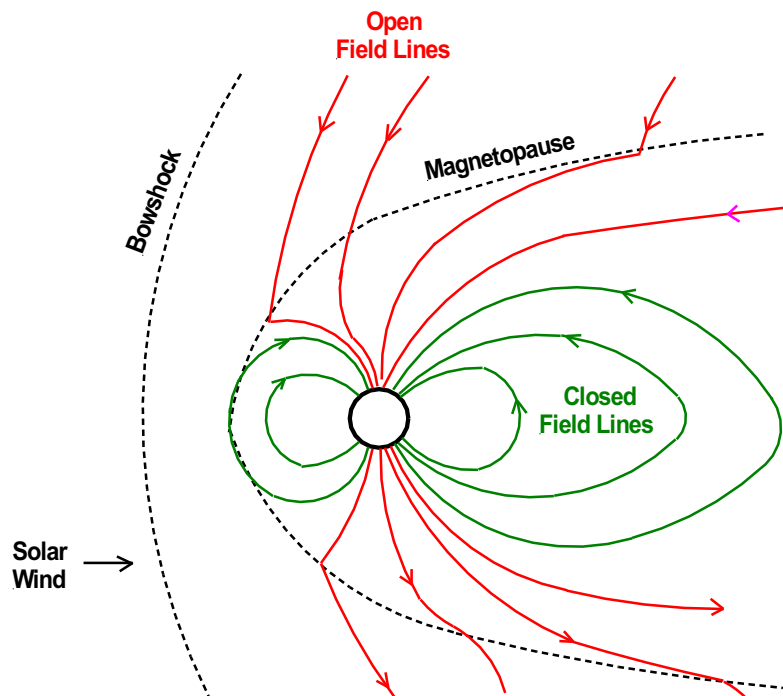


Figure 43 Closed and Open Magnetic Field Lines (source: author)

9.6 Ionization of Earth's Upper Atmosphere by Energetic Charged Particles

At mid and low-latitudes the main source of ionization in the upper atmosphere is X-ray and EUV (Extreme Ultra Violet) radiation from the Sun. X-ray and EUV radiation is also responsible for ionization at high latitudes. However, at high latitudes additional ionization results from energetic particles spirally around magnetic field lines downward into the polar region atmosphere. At times high energy particles are the primary form of high latitude ionization.

The high energy particles consist of:

- High energy electrons, and
- High energy protons and α – particles (helium nuclei).

9.6.1 Ionization by High Energy Electrons

In addition to X-ray and EUV radiation, neutral gas particles in the polar region are ionized by collisions with energetic electrons.

The collisions occur as incoming electrons, spiraling along magnetic field lines, enter the upper atmosphere. A collision can have two consequences:

1. The gas particle with which the incoming electron collides can be excited to a higher energy level.
2. The gas particle can actually be ionized by the collision.

In the first case most of the kinetic energy of a fast moving electron is lost when it collides with a gas particle. A gas particle is huge, typically 20,000 times more massive than an electron. The lost energy is absorbed by the particle exciting it to a higher energy level. In a second or two the particle dissipates the energy as photons of light and returns to its normal energy level. This is the type of collision responsible for auroral light displays.

In the second case the kinetic energy of the incoming electron is high enough to knock an electron out of a gas particle. The collision ionizes the gas particle and doubles the number of free electrons. The free electrons consist of the original incoming electron plus the electron stripped from the gas particle. Collisions of this type increase the E region electron density and thus the E region critical frequency.

The collisions also increase E layer conductivity permitting the intense auroral electrojet to flow in the polar E region. The electrojet disrupts the geomagnetic field in the auroral zone causing it to

vary wildly with the visual auroral display. The electrojet is thus responsible for the magnetic aspects of an auroral substorm similar in concept to the equatorial ring current inducing global geomagnetic storms.

Collisions with high energy electrons also has a secondary ionization affect. A small amount of the energy involved in a collision is converted to X-rays. The X-rays penetrate deeper into the atmosphere than do the electrons. In the process, the X-rays ionization additional gas particles further down in the atmosphere typically at an altitude of 50 km or less.

The ionization rate due to the secondary X-rays is far less than that produced by the energetic electrons higher up in the atmosphere. However, it is often the primary form of ionization at altitudes below 50 km.

9.6.2 Ionization by High Energy Protons

Upon arrival at Earth, high energy protons and α – particles from the Sun spiral downward along magnetic field lines into the polar region. As they do so they collide with neutral gas particles present in the upper atmosphere. If a collision is violent enough, a gas particle will be ionized.

High energy particles are typically ejected from the Sun by solar flares, coronal mass ejections, and coronal holes. These particles have significantly more energy than energetic electrons and consequently produce much higher levels of ionization in the E and D regions of the ionosphere.

Energetic protons, primarily from flares, are responsible for Polar Cap Absorption events (PCAs). During a PCA HF radio signals are absorbed throughout the polar region severely disrupting radio communications for several days.

9.7 Occurrence of Geomagnetic Storms

The occurrence and intensity of geomagnetic storms vary with the eleven-year solar cycle. The greatest number of storms typically occur during the declining phase of the solar cycle, a year or two following solar maximum (Figure 44). These storms are primarily coronal hole – CIR storms driven by high speed coronal hole wind (Figure 45). In addition, over half of large storms occur around the equinoxes, that is in March through April and September through October, when the geomagnetic field is favorably aligned with the IMF field. For the purposes of the graph in Figure 44, a geomagnetic disturbance is defined as a day on which the Ap index (see Section 14.9.2) equals, or exceeds, a value of 25. The graph shows the number of such days each year.

While solar wind speed and density are factors, the orientation of the solar wind magnetic field has the greatest impact on the severity of geomagnetic storms, or if storms will occur at all. Geomagnetic storms, including the largest storms, are most likely to develop when the B_z component of the solar wind IMF field is directed southward ($-B_z$), connecting with the northward geomagnetic field. Relatively few storms develop when the IMF field is pointed northward.

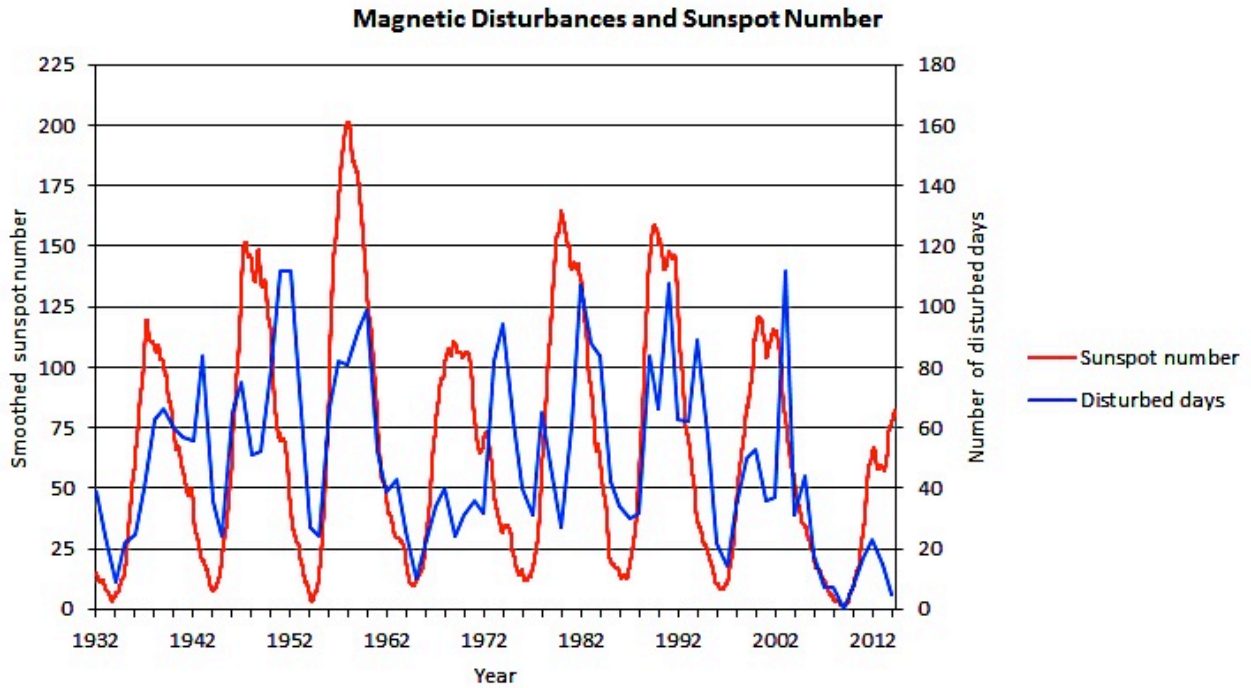


Figure 44 Magnetic Storm Intensity vs Solar Cycle (source: Space Weather Services)

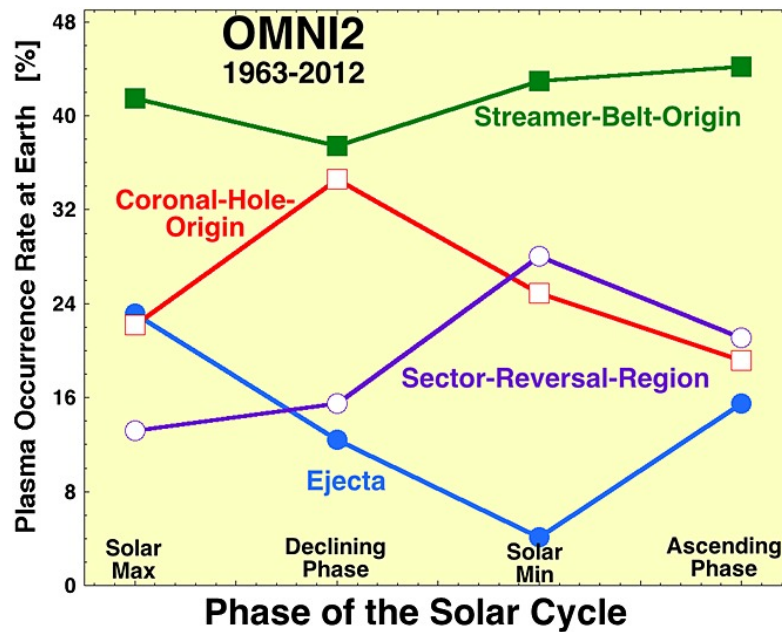


Figure 45 Occurrence of Solar Winds Throughout the solar cycle (source: Xu & Borovsky)

Solar Cycle Phase	Slow Streamer Belt Winds	Very Slow Sector Reversal Winds	Coronal Mass Ejection Winds	Fast Coronal Hole Winds	Geo-magnetic Storms	Substorms
Minimum	Ambient continuous background winds	High rate of occurrence	Rare	Average occurrence rate	Low rate of occurrence	1 substorm every 2 – 3 days
Ascending	Ambient continuous background winds	Average occurrence rate	Average occurrence rate	Low occurrence rate	Small increase in occurrence	Small increase in occurrence
Maximum	Ambient continuous background winds	Infrequent	High rate of occurrence	Average occurrence rate	Significant increase in occurrence	Significant increase in occurrence
Declining	Ambient continuous background winds	Average occurrence rate	Average occurrence rate	Very High rate of occurrence	High rate of occurrence	4 substorms per day

Table 2 Impact of the various types of solar winds on geomagnetic storms and substorms

Solar Minimum: This is the quiet period of the solar cycle with few sunspots and low solar activity. During solar minimum winds consist primarily of very slow sector reversal and slow streamer belt winds (Figure 45 and Table 2). These slow speed winds account in part for the low occurrence of geomagnetic storms and substorms during solar minimum. Slow speed winds can generate geomagnetic storms if the IMF magnetic field is directed southward. But the occurrence rate and intensity of such storms is low. Coronal hole wind can also occur during solar minimum and this wind can occasionally produce coronal hole - CIR storms. Typically, one substorm occurs about every 2 or 3 days during solar minimum. In contrast substorms occur at a rate of about 4 per day during the declining phase of the solar cycle when coronal hole - CIR storms are most pervasive. Coronal hole wind is the second most frequent type of solar wind, second only to slow streamer belt wind. The occurrence of CME storms is rare during solar minimum.

Ascending Phase: A few coronal mass ejections begin appearing during the ascending phase of the solar cycle resulting in a small increase in geomagnetic activity. Coronal hole wind is at its lowest level during this phase of the solar cycle, but is still significant with its rate of occurrence about the same as CME wind (Figure 45).

Solar Maximum: Solar maximum is the most active period of the solar cycle with large numbers of sunspots, high levels of EUV and x-ray radiation, solar prominences, large coronal loops, and frequent solar flares. Coronal mass ejects occur often during solar maximum resulting in a significant increase in geomagnetic storms and substorms. CME driven geomagnetic storms are the predominate type of magnetic storms during solar maximum with coronal hole - CIR storms being second.

Declining Phase: As described above, the largest number of storms typically occur during the declining phase of the solar cycle, a year or two following solar maximum. These are primarily coronal hole - CIR storms. Four substorms typically occur each day during the declining phase.

9.8 Phases of a Geomagnetic Storm

A typical magnetic storm consists of three phases as shown in Figure 46.

- Initial phase: an increase in the intensity of the geomagnetic field lasting only a few hours.
- Main phase: a large decrease in magnetic field strength dropping to its lowest level in several hours to a day.
- Recovery phase: a slow recovery to pre-storm conditions over a period of several days.

The initial phase of a CME geomagnetic storm often begins with a sudden increase in magnetic field intensity. The positive spike in field strength, known as sudden commencement, occurs almost simultaneously (within minutes) everywhere on Earth. It is caused by arrival of dense high speed solar wind that drives the bow shock closer to the Earth, compressing the magnetosheath and magnetosphere in the process.

Not all storms have an initial phase. In general, coronal hole – CIR storms do not produce a sudden commencement pulse. The reverse is also true. A sudden commencement can occur without initiating a magnetic storm if the IMF associated with a CME wind is directed northward. In this case the sudden commencement still occurs as the bow shock is driven toward the Earth but a subsequent storm fails to develop because the IMF does not connect to the geomagnetic field. Such an event is known as a Sudden Impulse. Finally, a sudden commencement will nearly always be followed by a magnetic storm if the IMF is pointed southward.

The main phase occurs as a strong southward IMF connects with the northward directed geomagnetic field. The connection peels open the geomagnetic field lines over the polar regions allowing a flood of solar wind charged particles to flow down the field lines into Earth's inner magnetosphere. The inflow increases the strength of the equatorial ring current and its associated magnetic field. Since the ring current magnetic field opposes the geomagnetic field, an increase in ring current produces the sharp negative spike in the geomagnetic field (Figure 46), resulting in a geomagnetic storm. How strong the storm is depends on the speed and particle density of the solar wind at the time.

The recovery phase is the longest duration phase of a magnetic storm. It is simply recovery of the magnetic field to pre-existing conditions as the ring current decays.

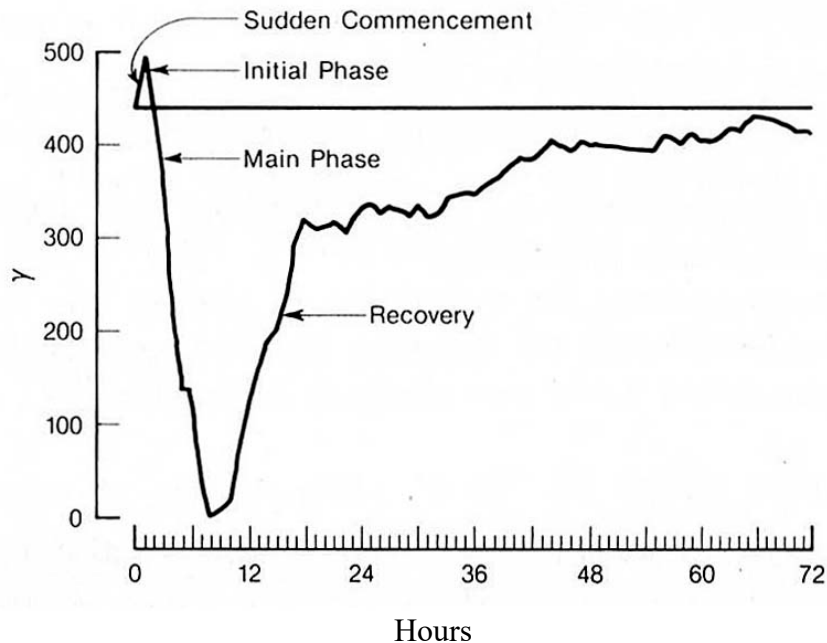


Figure 46 Phases of a Magnetic Storm (source: Davies)

9.9 Geomagnetic Indices

Geomagnetic activity is measured by a number of indices. These include:

- Disturbance Storm Time (Dst) index, and
- Kp and Ap indices.

9.9.1 Disturbance Storm Time Index

The Disturbance Storm Time (Dst) index measures the magnetic field strength of the equatorial ring current. An increase in the ring current produces a worldwide depression in the horizontal component of Earth's magnetic field, causing a geomagnetic storm.

The Dst index is compiled from hourly averages of the horizontal component of Earth's magnetic field recorded at four low latitude observatories. The observatories are located at Kakioka Japan, Honolulu Hawaii, San Juan Puerto Rico, and Hermanus South Africa.

The Dst index is zero on geomagnetic quiet days. An index of -50 or greater indicates a storm-level disturbance in the magnetic field. An index of -200 or deeper signifies a severe storm that can cause considerable damage and produce aurorae visible as far south as Washington D. C. Notice that a negative Dst number, for example -50, when added to Earth's positive core magnetic field results in a decrease in total magnetic field strength. In fact, the magnitude of the Dst index in nT (nano - tesla) is the strength of the ring current magnetic field. The Dst index is used by government agencies, satellite operators, power grid engineers, and others to analyze the strength and duration of geomagnetic storms.

Figure 47 shows the Dst index for March 1989. March 13th of that year was one of the most severe geomagnetic storms experienced in recent decades. The storm was so intense that it knocked out the Hydro Quebec electric power distribution system causing over 6 million people to lose electricity. Notice in this figure that the magnetic field spiked down -600 nT on the 13th of March.

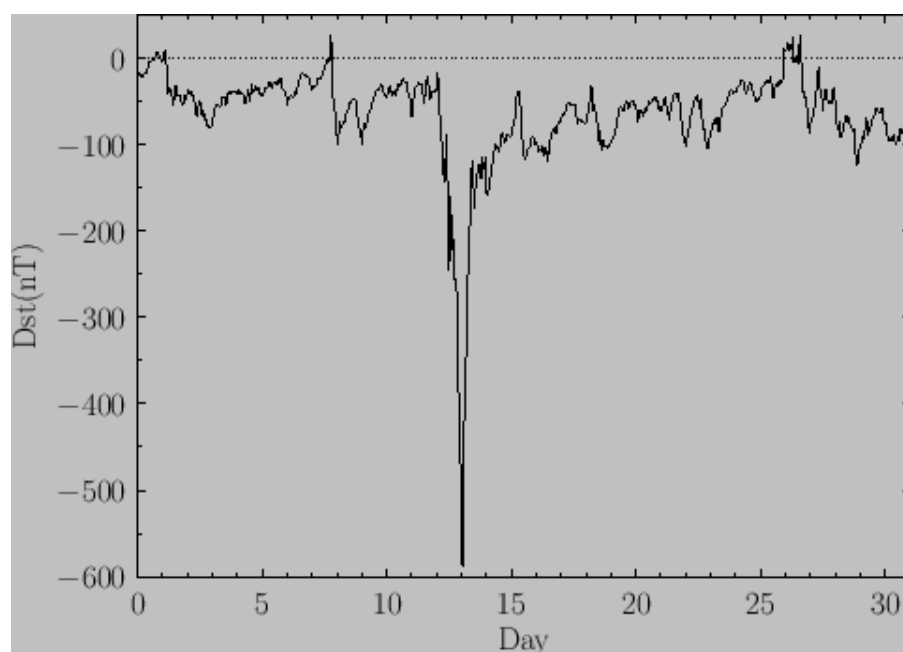


Figure 47 Dst index for the month of March 1989 (source: Farside.ph.utexas.edu)

The current Dst level can be obtained by clicking on Dst Index under the Current Conditions tab of the www.skywave-radio.org website.

9.9.2 Planetary K – index (K_p)

The planetary K – index is a measure of geomagnetic activity. That is, whether the Earth’s magnetic field is quiet (low K_p value), moderately active (medium K_p value), or experiencing a geomagnetic storm (high K_p value).

K_p is obtained by averaging together the amplitude and phase of the magnetic field measured over a 3 hour period. The measurements are performed at 12 magnetic field observatories around the world. The observations from the various observatories are combined together to provide the planetary K_p value. The value of K_p for each 3 hour period ranges from 0 (very quiet) to 9 (very disturbed) on a quasi-logarithmic scale. Values of K_p for September 27 through 30, 2020 are shown in Figure 48.

The Sun’s rotational period sometimes cause K_p values to recur every 27 days. This happens most frequently during the declining phase of a solar cycle when long duration coronal hole winds sweeping past Earth are most prevalent.

A_p is a daily index obtained from the same basic K_p data which then is converted to a linear scale and averaged over a full day in Universal Time. The range of values for the K_p and A_p indices are shown in Table 3. Notice in Figure 48 that green bars ($K_p < 4$) indicate quiet to active geomagnetic conditions. Yellow bars ($K_p = 4$) signify minor storms and red bars ($K_p > 4$) indicate major to severe storms.

The current K_p index value can be obtained by clicking on K_p Index under the Current Conditions tab of the www.skywave-radio.org website.

K_p	A_p		A_p	Geomagnetic Activity
0	0		0 - 7	Quiet
1	3			
2	7		8 – 15	Unsettled
3	15		16 - 29	Active
4	27		30 - 49	Minor Storm
5	48		50 - 99	Major Storm
6	80			
7	140		> 100	Severe Storm
8	240			
9	400			

Table 3 K_p and A_p Indices

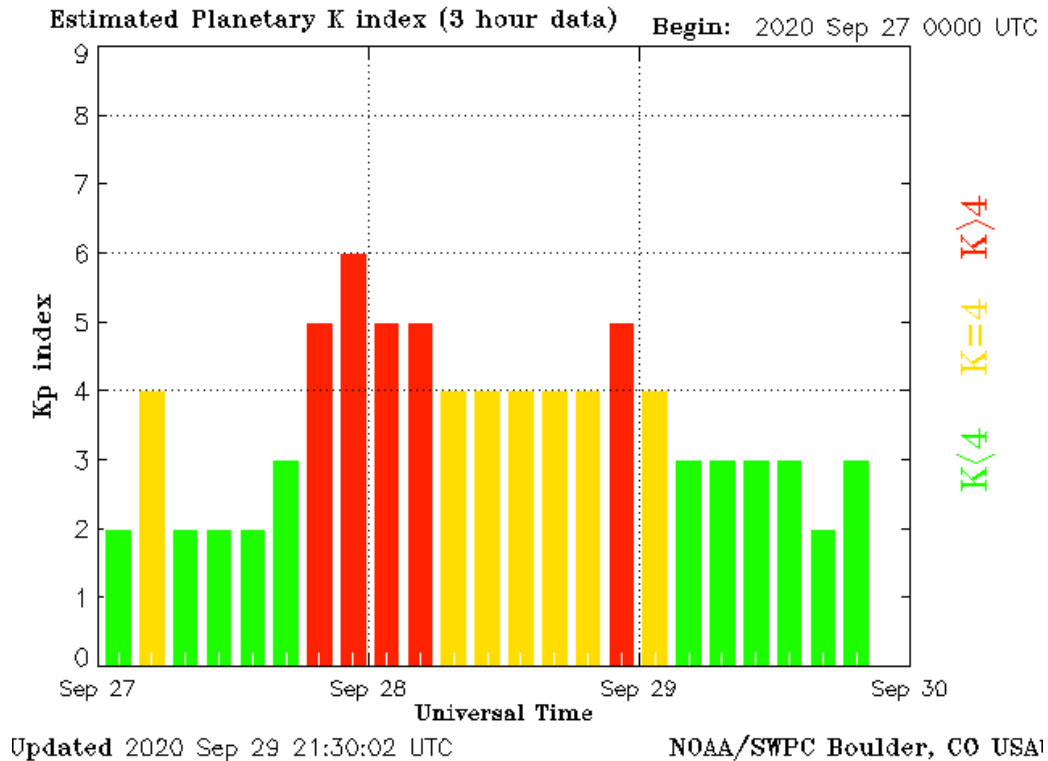


Figure 48 K_p Values for September 27 – 30, 2020

9.10 Effects of Geomagnetic Storms

What are the ramifications of a geomagnetic storm? Large geomagnetic storms can:

- Seriously disrupt electric power distribution systems,
- Induce dangerous electrical currents in long pipelines,
- Increase satellite drag, and
- Produce bright aurora.

The second largest magnetic storm on record occurred on March 13, 1989. This storm was extensively studied by J. A. Joslyn, R. D. Hunsucker, and others. The A_p index for the storm was 246, the second largest A_p value in the 57 years since the index began in 1932. The aurora produced by the storm was visible as far south as Florida, Mexico, and Grand Cayman Island. The storm continued for nearly two days. Toward the end of the storm, the auroral electrojet was flowing south

of Fredericksburg, Virginia at a latitude of 49° N instead of in the auroral zone (at magnetic latitude $65^\circ - 75^\circ$ N) where it is normally found.

The intense solar wind, ~ 30 times greater than normal, compressed the magnetopause from $11 R_E$ (Earth radii) to $4.7 R_E$. For a period of time the GOES - 6 and GOES - 7 satellites, as well as other satellites in geosynchronous orbits $6.6 R_E$ from Earth, were outside the magnetosphere in the full fury of the solar wind. The GOES satellites (Figure 49) continuously monitor Earth's magnetic field, solar X-ray and EUV radiation, and a variety of other geophysical parameters.

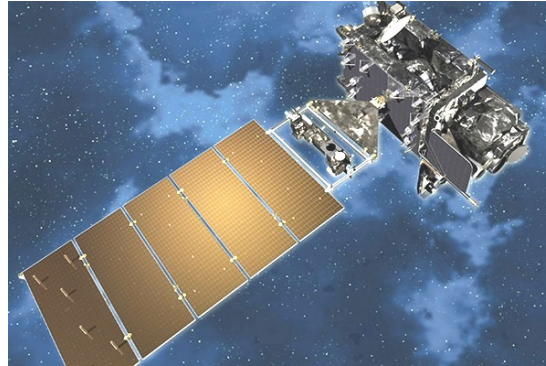


Figure 49 GOES 16 Spacecraft (Source: NOAA)

In addition to compressing the magnetosphere, the storm heated Earth's upper atmosphere causing it to expand outward increasing the drag on satellites orbiting the Earth. In general, increased drag resulting from magnetic storms accelerates the rate of satellite orbital decay causing them to re-enter the atmosphere sooner than expected.

The most serious impact of the storm, however, was its disruption of electric power distribution in Canada. Fluctuations in the geomagnetic field induce electrical currents in long distance power lines. These fluctuations cause voltage surges which saturate power transforms and trip protective relays. This is exactly what occurred on March 13 in the Quebec electric power system which lost power for 9 hours. Users in north-eastern United States were also affected.

The same conditions causing the geomagnetic storm also triggered an ionospheric storm. During the day of March 13 mid-latitude electron densities and critical frequencies remained at night time levels. The equatorial ionosphere essentially disappeared while the polar ionosphere was considerably disrupted making HF radio communications impossible over large regions of Earth.

Space weather conditions responsible for geomagnetic and ionospheric storms are continuously monitored by the National Oceanic and Atmospheric Administration (NOAA) using a fleet of spacecraft in Earth orbit as well as in orbit around the Sun. NOAA summarize space weather conditions in three categories:

G: Geomagnetic Storms

S: Solar Radiation

R: Radio Blackouts

9.10.1 NOAA Geomagnetic Activity Summary

NOAA categorizes geomagnetic storms using the G1 – G5 scale summarized in Table 4 below. The scale is based on the planetary K – index (K_p). Typical K_p measurements over a five day period are shown in Figure 48 above. Current K_p value can be obtained by clicking on K_p Index under the Current Conditions tab of the www.skywave-radio.org website while the NOAA geomagnetic activity value is found on the NOAA Space Weather Enthusiasts Dashboard by clicking on Space Weather Conditions under the Current Conditions tab of the same website.

9.10.2 NOAA Solar Radiation Storm Summary

Solar radiation storms occur when large prominences and coronal loops collapse accelerating charged particles, primarily protons, to nearly the speed of light. At these velocities protons can traverse the 150 million kilometer distance from the Sun to Earth in only a few tens of minutes. When they reach Earth the fast moving protons penetrate the magnetosphere and spiral down magnetic field lines into the polar regions of Earth's upper atmosphere. Often these collapses cause solar flares and associated coronal mass ejections (CME).

NOAA categorizes Solar Radiation Storms using the S1 – S5 scale summarized in Table 5. The scale is based on measurements of energetic protons taken by the GOES satellite in geosynchronous orbit. The start of a Solar Radiation Storm is defined as the time when the flux of protons at energies ≥ 10 MeV equals or exceeds 10 proton flux units (pfu). The end of a Solar Radiation Storm is defined as the last time when the flux of ≥ 10 MeV protons was measured at or above 10 pfu. This definition allows multiple injections from flares and interplanetary shocks to be encompassed by a single Solar Radiation Storm. A Solar Radiation Storm can persist for time periods ranging from hours to days.

Solar Radiation Storms can cause a number of problems. When energetic protons collide with satellites or humans in space, they can penetrate deep into the object they collide with causing damage to electronic circuits and biological DNA. During more extreme Solar Radiation Storms, passengers and crew in high flying aircraft at high latitudes may be exposed to radiation risk. Also, when the energetic protons collide with the atmosphere, they ionize atoms and molecules in the lower part of the ionosphere (in the D region) increasing the absorption of High Frequency (HF) radio waves making radio communication difficult or impossible.

The GOES Proton Flux data for June 2 through 5, 2022 is shown in Figure 50. Notice in Figure 50 that the 10 MeV storm threshold is shown on the graph. Current proton flux data can be obtained by clicking on Proton Flux under the Current Conditions tab of the www.skywave-radio.org website while the NOAA Solar Radiation Storm value is found on the NOAA Space Weather Enthusiasts Dashboard by clicking on Space Weather Conditions under the Current Conditions tab of the same website.

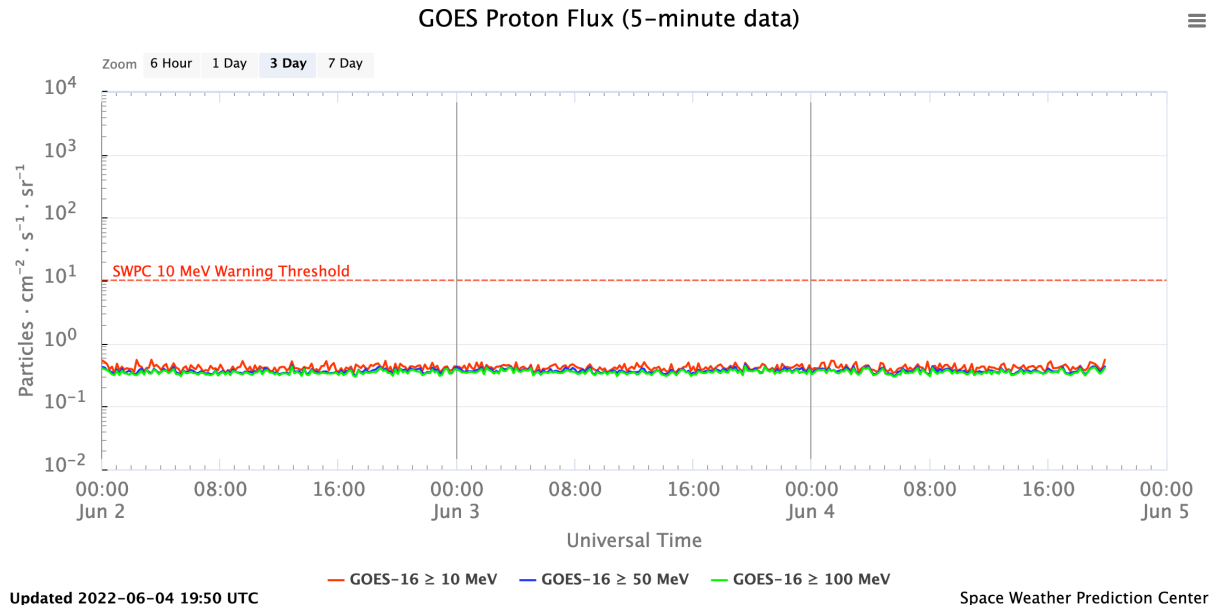


Figure 50 GOES Proton Flux (source: Space Weather Prediction Center)

9.10.3 NOAA Radio Blackout Summary

Radio blackouts result from solar flares eruptions generally associated with the catastrophic collapse of large prominences and coronal loops. A solar flare releases a massive amount of energy in the form of gamma rays, x-rays, and visible light. The copious amounts of x-rays travel from the Sun to Earth in 8 minutes heavily ionizing the D layer of the ionosphere.

Solar flare intensities are classified in terms of peak emission in the 0.1 – 0.8 nm spectral band (soft x-rays). Level “A” is defined as the lowest X-ray flux level with a flux of 10⁻⁸ W/m². The next level, ten times higher, is level “B” (≥ 10⁻⁷ W/m²); followed by “C” flares (10⁻⁶ W/m²), “M” flares (10⁻⁵ W/m²), and finally “X” flares (10⁻⁴ W/m²). The x-ray flux level for June 5 – 8, 2022 is shown in Figure 51. Current x-ray flux data can be obtained by clicking on X-ray Flux under the Current Conditions tab of the www.skywave-radio.org website.

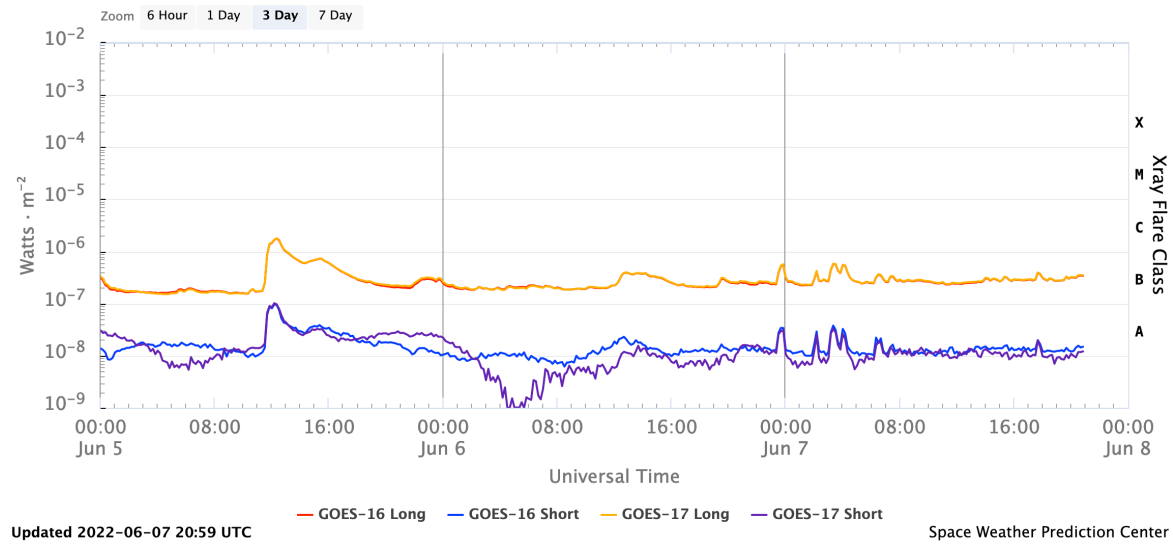


Figure 51 Solar X-ray flux (source: Space Weather Prediction Center)

NOAA categorizes Radio Blackouts using the R1 – R5 scale summarized in Table 6. The scale is based on measurements of solar x-ray flux taken by the GOES satellite in geosynchronous orbit. The NOAA scale corresponds to the following X-ray Flux levels:

- R1 = Minor M1 level
- R2 = Moderate M5
- R3 = Strong X1
- R4 = Severe X10
- R5 = Extreme X20

Scale	Descriptor	Geomagnetic Storms
G5	Extreme $K_p = 9$	<p>Power systems: widespread voltage control problems and protective system problems can occur, some grid systems may experience complete collapse or blackouts. Transformers may experience damage.</p> <p>Spacecraft operations: may experience extensive surface charging, problems with orientation, uplink/downlink and tracking satellites.</p> <p>Other systems: pipeline currents can reach hundreds of amps, HF (high frequency) radio propagation may be impossible in many areas for one to two days, satellite navigation may be degraded for days, low-frequency radio navigation can be out for hours, and aurora has been seen as low as Florida and southern Texas (typically 40° geomagnetic lat.).</p>
G4	Severe $K_p = 8$	<p>Power systems: possible widespread voltage control problems and some protective systems will mistakenly trip out key assets from the grid.</p> <p>Spacecraft operations: may experience surface charging and tracking problems, corrections may be needed for orientation problems.</p> <p>Other systems: induced pipeline currents affect preventive measures, HF radio propagation sporadic, satellite navigation degraded for hours, low-frequency radio navigation disrupted, and aurora has been seen as low as Alabama and northern California (typically 45° geomagnetic lat.).</p>
G3	Strong $K_p = 7$	<p>Power systems: voltage corrections may be required, false alarms triggered on some protection devices.</p> <p>Spacecraft operations: surface charging may occur on satellite components, drag may increase on low-Earth-orbit satellites, and corrections may be needed for orientation problems.</p> <p>Other systems: intermittent satellite navigation and low-frequency radio navigation problems may occur, HF radio may be intermittent, and aurora has been seen as low as Illinois and Oregon (typically 50° geomagnetic lat.).</p>
G2	Moderate $K_p = 6$	<p>Power systems: high-latitude power systems may experience voltage alarms, long-duration storms may cause transformer damage.</p> <p>Spacecraft operations: corrective actions to orientation may be required by ground control; possible changes in drag affect orbit predictions.</p> <p>Other systems: HF radio propagation can fade at higher latitudes, and aurora has been seen as low as New York and Idaho (typically 55° geomagnetic lat.).</p>
G1	Minor $K_p = 5$	<p>Power systems: weak power grid fluctuations can occur.</p> <p>Spacecraft operations: minor impact on satellite operations possible.</p> <p>Other systems: migratory animals are affected at this and higher levels; aurora is commonly visible at high latitudes (northern Michigan and Maine).</p>

Table 4 NOAA Geomagnetic Storm Classification

Scale	Descriptor	Solar Radiation Storms
S5	Extreme	<p><u>Biological</u>: unavoidable high radiation hazard to astronauts on EVA (extra-vehicular activity); passengers and crew in high-flying aircraft at high latitudes may be exposed to radiation risk.</p> <p><u>Satellite operations</u>: satellites may be rendered useless, memory impacts can cause loss of control, may cause serious noise in image data, star-trackers may be unable to locate sources; permanent damage to solar panels possible.</p> <p><u>Other systems</u>: complete blackout of HF (high frequency) communications possible through the polar regions, and position errors make navigation operations extremely difficult.</p>
S4	Severe	<p><u>Biological</u>: unavoidable radiation hazard to astronauts on EVA; passengers and crew in high-flying aircraft at high latitudes may be exposed to radiation risk.</p> <p><u>Satellite operations</u>: may experience memory device problems and noise on imaging systems; star-tracker problems may cause orientation problems, and solar panel efficiency can be degraded.</p> <p><u>Other systems</u>: blackout of HF radio communications through the polar regions and increased navigation errors over several days are likely.</p>
S3	Strong	<p><u>Biological</u>: radiation hazard avoidance recommended for astronauts on EVA; passengers and crew in high-flying aircraft at high latitudes may be exposed to radiation risk.</p> <p><u>Satellite operations</u>: single-event upsets, noise in imaging systems, and slight reduction of efficiency in solar panel are likely.</p> <p><u>Other systems</u>: degraded HF radio propagation through the polar regions and navigation position errors likely.</p>
S2	Moderate	<p><u>Biological</u>: passengers and crew in high-flying aircraft at high latitudes may be exposed to elevated radiation risk.</p> <p><u>Satellite operations</u>: infrequent single-event upsets possible.</p> <p><u>Other systems</u>: effects on HF propagation through the polar regions, and navigation at polar cap locations possibly affected.</p>
S1	Minor	<p><u>Biological</u>: none.</p> <p><u>Satellite operations</u>: none.</p> <p><u>Other systems</u>: minor impacts on HF radio in the polar regions</p>

Table 5 NOAA Solar Radiation Storm Classification

Scale	Descriptor	Radio Blackouts
R5	Extreme GOES X-ray flux X20	<u>HF Radio</u> : Complete HF (high frequency) radio blackout on the entire sunlit side of the Earth lasting for a number of hours. This results in no HF radio contact with mariners and en-route aviators in this sector. <u>Navigation</u> : Low-frequency navigation signals used by maritime and general aviation systems experience outages on the sunlit side of the Earth for many hours, causing loss in positioning. Increased satellite navigation errors in positioning for several hours on the sunlit side of Earth, which may spread into the night side.
R4	Severe X10	<u>HF Radio</u> : HF radio communication blackout on most of the sunlit side of Earth for one to two hours. HF radio contact lost during this time. <u>Navigation</u> : Outages of low-frequency navigation signals cause increased error in positioning for one to two hours. Minor disruptions of satellite navigation possible on the sunlit side of Earth.
R3	Strong X1	<u>HF Radio</u> : Wide area blackout of HF radio communication, loss of radio contact for about an hour on sunlit side of Earth. <u>Navigation</u> : Low-frequency navigation signals degraded for about an hour.
R2	Moderate M5	<u>HF Radio</u> : Limited blackout of HF radio communication on sunlit side of the Earth, loss of radio contact for tens of minutes. <u>Navigation</u> : Degradation of low-frequency navigation signals for tens of minutes.
R1	Minor M1	<u>HF Radio</u> : Weak or minor degradation of HF radio communication on sunlit side of the Earth, occasional loss of radio contact. <u>Navigation</u> : Low-frequency navigation signals degraded for brief intervals.

Table 6 NOAA Radio Blackout Classification

Current space weather conditions can be found on the NOAA Space Weather Enthusiasts Dashboard by clicking on Space Weather Conditions under the Current Conditions tab of the www.skywave-radio.org website

References

Hunsucker, R. D. and Hargreaves, J.K.; “The High-Latitude Ionosphere and its Effects on Radio Propagation”; Cambridge University Press, 2003

Campbell, Wallace H.; “Introduction to Geomagnetic Fields”; Cambridge University Press, 2003

Davies, Kenneth; “Ionospheric Radio”; Peter Peregrinus Ltd., 1990

McNamara, Leo F.; “The Ionosphere: Communications, Surveillance, and Direction Finding”; Krieger Publishing Company, 1991

Goodman, John M.; “Space Weather & Telecommunications”; Springer Science + Business Media Inc., 2005

Levis, Curt A. ; Johnson, Joel T.; and Teixeira, Fernando L.; “Radiowave Propagation Physics and Applications”; John Wiley & Sons, Inc., 2010

Nichols, Eric P.; “Propagation and Radio Science”; The American Radio Relay League, Inc. 2015

Cander, Ljiljana R.; “Ionospheric Space Weather”; Springer Geophysics 2019

Khazanov, George V.; “Space Weather Fundamentals”; National Aeronautics and Space Administration, 2016

DeSoto, Clinton B., “200 Meters & Down”; The American Radio Relay League, Inc., 1936

Yeang, Chen-Pang; “Probing The Sky With Radio Waves”; The University of Chicago Press, 2013

Devoldere, John; “Low-Band DXing” fourth edition; ARRL, 2005

“The ARRL Antenna Book For Radio Communications”; ARRL

Foukal, Peter; “Solar Astrophysics third edition”; Wiley-VCH Publishing Company, 2013

Carroll, Bradley W. and Ostlie, Dale A.; “An Introduction to Modern Astrophysics”; Addison-Wesley Publishing Company Inc., 1996

Golub, Leon and Pasachoff, Jay M.; “Nearest Star The Surprising Science of Our Sun second edition”; Cambridge University Press, 2014

Moldwin, Mark; “An Introduction to Space Weather”; Cambridge University Press, 2008

Loff, Sarah: ”Explorer and Early Satellites”; National Aeronautics and Space Administration, Aug 3, 2017

“Solar experts predict the Sun’s activity in Solar Cycle 25 to be below average, similar to Solar Cycle 24”; 2019 NOAA Space Weather Workshop in Boulder, Colo.

Minzner, R. A.; “The 1976 Standard Atmosphere Above 86 km Altitude” NASA Goddard Space Flight Center, 1976

Ahrens, C. Donald; “Essentials of Meteorology”; Wadsworth Publishing Company, 1998